Zoological Studies **63:**25 (2024)

Population Genetics of the Deep-sea Acorn Barnacle *Bathylasma hirsutum* (Hoek, 1883) and the First Report of its Affiliation with a Hydrothermal Vent Field

Jenny Neuhaus[1,*], Katrin Linse[2], Saskia Brix[1], Pedro Martínez Arbizu[3], and James Taylor[1,4]

[1]*German Centre for Marine Biodiversity Research (DZMB), c/o Biozentrum Grindel, Martin-Luther-King-Platz 3, 20146 Hamburg, Germany.* [*]*Correspondence: E-mail: jenny.neuhaus@senckenberg.de (Neuhaus) E-mail: saskia.brix-elsig@senckenberg.de (Brix)*

[2]*British Antarctic Survey, Natural Environmental Research Council, High Cross, Madingley Road, Cambridge CB3 0ET, UK. E-mail: kl@bas.ac.uk (Linse)*

[3]*German Centre for Marine Biodiversity Research (DZMB), Senckenberg am Meer, Südstrand 44, 26382, Wilhelmshaven, Germany. E-mail: pedro.martinez@senckenberg.de (Arbizu)*

[4]*GEOMAR Helmholtz Centre for Ocean Research, 24105 Kiel, Germany. E-mail: jtaylor@geomar.de (Taylor)*

ORCiD:
Jenny Neuhaus: https://orcid.org/0009-0000-7570-4094

(Received 1 December 2023 / Accepted 10 April 2024 / Published -- 2024)
Communicated by Benny K.K. Chan

Confined by the Mid-Atlantic Ridge and the European continental shelf, the deep-sea acorn barnacle *Bathylasma hirsutum* (Hoek, 1883) lives in the northeast Atlantic deep sea where it has been frequently reported from high current areas. Cemented to a solid substrate during its entire adult life, the species can only disperse by means of planktotrophic nauplius larvae. This study reports on the occurrence, ecology and genetic connectivity of *B. hirsutum* from four sites within the northeastern Iceland Basin and presents a first record of the species living affiliated a hydrothermal vent field on the Reykjanes Ridge axis. Vent-associated specimens were found to differ extrinsically from their natural shaded conspecifics by a prominent brown-black shell precipitate. Energy Dispersive Spectroscopy revealed ferromanganese oxides to be the main component of these shell precipitates. Morphometric measurements of shell plates revealed specimens from the vent-associated habitat to be smaller compared to non-venting sites. Molecular species delimitation based on the mitochondrial *COI* and nuclear EF1 genetic markers aided species identification and revealed a low intraspecific genetic variability. Our findings suggest a pronounced genetic connectivity of *B. hirsutum* within the studied region and provide a first step towards a biogeographic study. As such, habitats of hydrothermal influence along the Mid-Atlantic Ridge are discussed upon as possible niches, as are deep-sea basins in the western Atlantic as potential habitats. In light of the reported affiliation with hydrothermal activity, we elaborate on the

potential for the sister species *Bathylasma corolliforme* (Hoek, 1883) and *Bathylasma chilense* Araya & Newman, 2018 to utilise equivalent habitats in the Antarctic and Pacific Ocean, respectively. Our record of the unacquainted ecological niche occupation for *B. hirsutum* emphasises the need for further research on bathylasmatid acorn barnacles along the extensive Mid-Atlantic Ridge where many biological communities remain to be discovered.

Key words: Bathylasmatidae, Biogeography, Connectivity, Habitat expansion, Larval distribution

Citation: Neuhaus J, Linse K, Brix S, Martínez Arbizu P, Taylor J. 2024. Population genetics of the deep-sea acorn barnacle *Bathylasma hirsutum* (Hoek, 1883) and the first report of its affiliation with a hydrothermal vent field. Zool Stud **63:**25.

BACKGROUND

During the past 30 years, more than sixty hydrothermal vent systems have been discovered along the Mid-Atlantic Ridge (MAR), known as the longest obliquely spreading section of the global mid-ocean ridge systems (Beaulieu and Szafrański 2020; Desbruyéres et al. 2000; Desbruyères et al. 2006; German et al. 1994; Taylor et al. 2021; Wheeler et al. 2013). Elaborate studies on dominant faunal compositions of MAR vent communities, such as polychaetes (Kongsrud et al. 2013; Shields and Blanco-Perez 2013; Sigvaldadóttir and Desbruyères 2003), bivalves (Cravo et al. 2007; Duperron et al. 2006; Ó Foighil et al. 2001), and anemones (Fabri et al. 2011; Fautin and Barber 1999; López-González et al. 2003; Van Dover 1995) have contributed extensively to better understand these fragile ecosystems and map their particular biodiversity (Biscoito et al. 2006; Boschen-Rose and Colaço 2021; Desbruyéres et al. 2000; Gebruk et al. 1997, 2010). The Reykjanes Ride represents a ~950 km long submarine continuation of the MAR with an axial depth ranging from the shoreline southwest of the volcanic Iceland Peninsular to more than 2000 m at the Bight Fracture Zone (Keeton et al. 1997; Searle et al. 1998; Fig. 1). Owed to erupted lava from volcanic seamounts, the ridge substrate is mainly composed of volcanic rock and pillow lava, providing hard-bottom habitats for a wide range of species. Until recently, the only recognised hydrothermal active field along this extensive ridge was the Steinahóll vent field (63°N) at ~300 m depth (German et al. 1994). Late bathymetric mapping and a detailed description of Steinahóll added another three vent sites to the list of hydrothermal activity in this fragile area (Taylor et al. 2021). Current research activities near 59°N lead to the discovery of yet another active vent field situated on the edge of a large, faulted seamount at ~650 m depth (Brix et al. 2020). Proximal to this

novel hydrothermal vent field on the Reykjanes Ridge, the deep-sea acorn barnacle *Bathylasma hirsutum* (Hoek, 1883) was found attached to several volcanic boulders. Unlike the presence of characteristic vent barnacles in hydrothermal systems of the Pacific and Indian Ocean, Herrera et al. (2015) inferred cirripedes to be generally absent from MAR hydrothermal vent systems. Our findings present the first record of a barnacle species associated with hydrothermal activity on the northern section of the MAR. At current, the two groups of barnacles associated with deep-sea hydrothermal vents encompass all members of the superfamily Neolepadoidea as well as three species of the balanomorph genus *Eochionealasmus* Yamaguchi, 1990 (Chan et al. 2021 2020; Yamaguchi and Newman 1990 1997a 1997b). We introduce a third group of balanomorph barnacle, the genus *Bathylasma* Newman & Ross, 1971, with at least one opportunist species occupying a hydrothermal habitat. Along with the species of study, the genus *Bathylasma* Newman & Ross, 1971 currently comprises three extant species, namely *B. alearum* (Foster, 1978), *B. chilense* Araya & Newman, 2018 and *B. corolliforme* (Hoek, 1883), distributed at depths of 37–2000 m from the coasts of New Zealand, Chile, and the Antarctic Peninsula, respectively (Araya and Newman 2018; Foster 1978; Meyer et al. 2021).

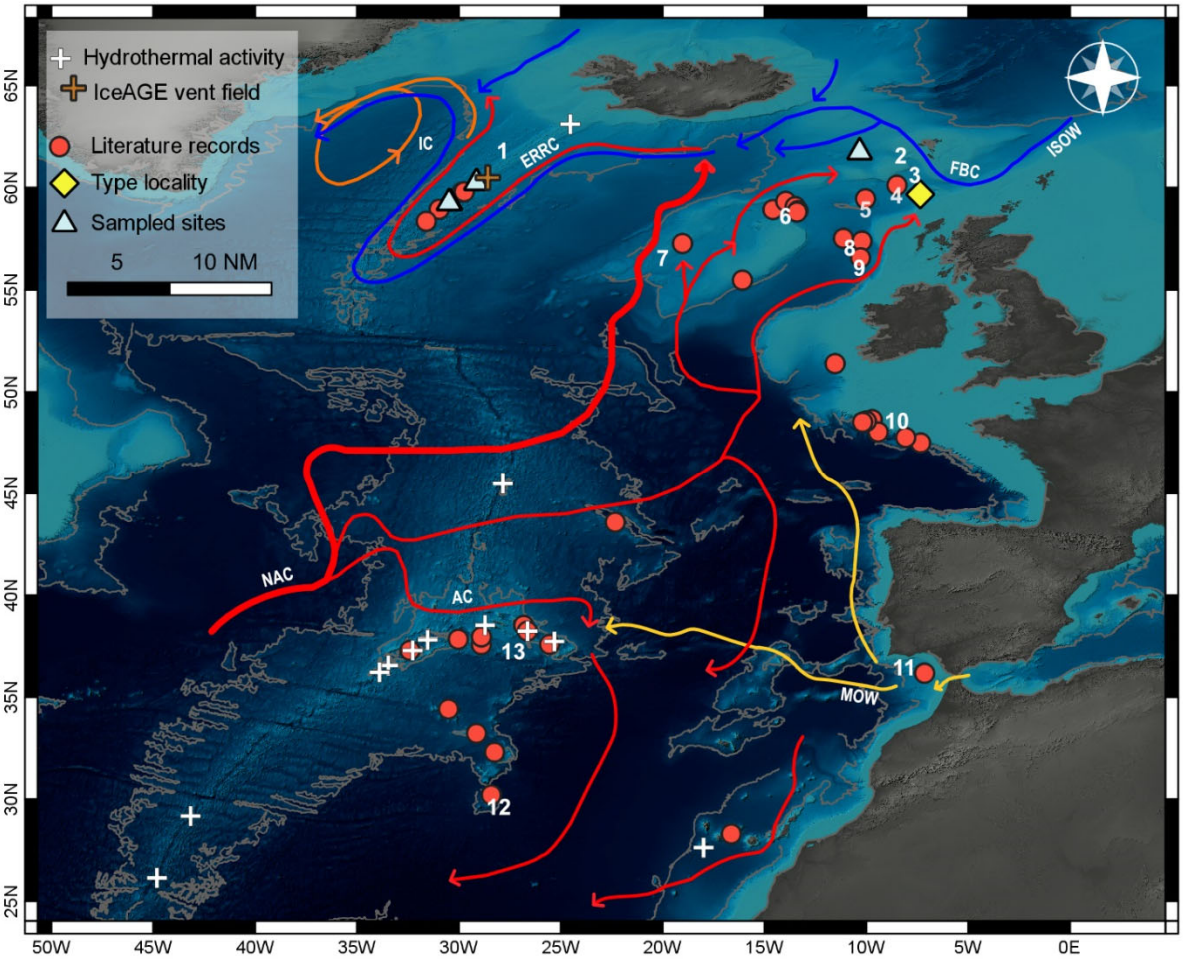

Fig. 1. Distributional range of the deep-sea acorn barnacle *Bathylasma hirsutum* in the north-east Atlantic. Literature records are included from the: (1) Reykjanes Ridge, (2) Faroe-Bank Channel, (3) Wyville Thomson Ridge, (4) Rockall Trough, (5) Rosemary Bank, (6) George Bligh Bank, (7) Hatton Bank, (8) Anton Dohrn Seamount, (9) Hebrides terrace, (10) Celtic Shelf, (11) Gulf of Cádiz, (12) Great Meteor Seamount, and (13) Azores Archipelago. Schematic of the main circulation patterns adapted from Koman et al. 2020 and Puerta et al. 2020. Red arrows depict surface waters of North Atlantic Current (NAC) origin, with a branch of the Azores Current (AC). Yellow arrows depict Mediterranean Outflow Water (MOW). Blue arrows indicate deep-water pathways of the Iceland Scotland Overflow Water (ISOW) flowing towards the Faroe Bank Channel (FBC), as well as overflow waters that run in parallel to the East Reykjanes Ridge Current (ERRC). Orange arrows represent surface waters of the Irminger Current (IC) with mixtures of Arctic and Atlantic waters.

Distributional range of *Bathylasma hirsutum*

Bathylasma hirsutum was first described from 944 m depth south of the Wyville Thomson Ridge (59°40'N 07°21'W; Hoek 1883). The species is nested within the family Bathylasmatidae Newman & Ross, 1971, which includes sole deep-sea species of six genera (Chan et al. 2021; Jones 2000; Newman and Ross 1971). In the history of the controversial position of the Bathylasmatidae, Jones (2000), based on their morphological characters, classified the genera *Hexelasma* Hoek, 1913 and *Bathylasma* under the Pachylasmatoidea (now Coronuloidea Leach, 1817). In Chan et al. (2017), molecular evidence suggested the clade of *Hexelasma* and *Bathylasma* to be sister to the Tetraclitidae Gruvel, 1903, nested within the same clade. Finally, the comprehensive molecular approach by Chan et al. (2021) suggested to treat Bathylasmatidae as a discrete family, nested within the Coronuloidea.

Bathylasma hirsutum has a distributional range bounded to the North-East (NE) Atlantic where it inhabits hard-bottom habitats in high current areas between 384–1829 m depth (Fig. 1). The species is known to occur along the Reykjanes Ridge (Copley et al. 1996; Murton et al. 1995; Poltarukha and Zevina 2006b), in addition to banks and seamounts in the Rockall Trough, being Rosemary Bank, George Bligh Bank, Hatton Bank, Anton Dohrn Seamount and Hebrides Terrace (Duineveld et al. 2007; Gage 1986; Narayanaswamy et al. 2006 2013; Young 2001). Further records extend to the south along the Celtic Shelf (Southward and Southward 1958; Young 1998) towards the Gulf of Cádiz (Foster and Buckeridge 1995) and near Tenerife (Gruvel 1903). Along the MAR, *B. hirsutum* has repeatedly been reported from the Azores Archipelago (Gruvel 1920; Poltarukha and Zevina 2006a; Southward 1998; Young 1998) as well as from the Great Meteor

Seamount (Poltarukha and Zevina 2006a; Young 2001). The species populates a wide range of substrates, such as dropstones (Duineveld et al. 2007), telegraph cables (Gruvel, 1903; Southward & Southward, 1958), echinoid spines (Hoek 1883; Southward and Southward 1958), as well as alive and dead coral (Southward, 1998). Furthermore, shell debris from dead barnacles that accumulates in the periphery of the substratum they are cemented to provides a solid layer, even on soft sediments, which can be re-populated by recruits (Bullivant and Dearborn 1967; Dayton et al. 1982; Foster and Buckeridge 1995; Gage and Tyler 1991).

Larval biology and shell growth

Cemented to a solid substrate during their entire adult life, barnacles can only disperse by means of larvae. In general, they develop through a maximum of six naupliar stages which are followed by metamorphosis into the terminal cypris stage (Dayton et al. 1982; Høeg and Møller 2006; Pineda et al. 2021; Walker et al. 1987). Adapted to respective habitats, cyprids show a broad array of sensory setae and attachment organs across species, facilitating them to sense the chemical environment (Bielecki et al. 2009; Maruzzo et al. 2012) and to bipedally move across the substratum (Lagersson and Høeg 2002; Walker et al. 1987; Yorisue et al. 2013 2016). Eventually, the cyprid induces the final cementation and develops into a juvenile sedentary barnacle (Aldred et al. 2018; Crisp 1955; DiBacco et al. 2011). In the deep sea, several species have developed a range of deviant larval development strategies (Yorisue et al. 2013). For example, some species directly hatch as cyprids which are immediately disposed to search for an attachment site (Buhl-Mortensen and Høeg 2006). Others, such as the endemic vent barnacle of the genus *Neoverruca* Newman 1989, develop lecithotrophic nauplii to ensure dispersal over far distances with a long larval development (Southward and Jones 2003). In addition, a special habitat adaptation in vent-barnacles speeds up the metamorphosis into the sensory cyprid as their ontogeny answers to elevated water temperatures (Watanabe et al. 2004 2006; Yorisue et al. 2013). Currently, nothing is known about the ontogeny of the deep-sea barnacle *B. hirsutum*. Single larval stages of the Antarctic *B. corolliforme* have been examined in specimens from the McMurdo Sound region (Dayton et al. 1982; Foster 1989). Due to their relatedness, the naupliar and cyprid anatomy is suggested to be comparable in both species. Besides their conventional balanomorph anatomy which is elaborated in Dayton et al. (1982) and Foster (1989), the larvae of *B. corolliforme* distinguish from other balanomorph species by having a naupliar eye and an overall larger size. According to Foster (1989), larval development likely exceeds three weeks to complete, comparable to the boreal species *Semibalanus balanoides* (Linnaeus, 1767) which is suggested to have a planktonic existence of 3–6 weeks (Barnes and Barnes 1959 1958). The cypris develops into an undivided chitinous

annulus with a single hirsute ring, including the aperture with terga and scuta adjacent to which a pair of photoreceptors is found (Dayton et al. 1982). Attachment, metamorphosis of settled cyprids and early post-larval mortality are the most critical steps and determine barnacle recruitment (Pineda et al. 2002; Thiyagarajan et al. 2002). As the barnacle grows, it produces distinct growth increments that undulate parallel to the basal margin and run continuously on the external of each of the parietal plate (Anderson 1994; Fig. 2). These increments are referred to as either growth lines (Checa et al. 2019; Varfolomeeva et al. 2008) or growth ridges (Anderson 1994; Blomsterberg et al. 2004; Bourget 1987; Bourget and Crisp 1975). With the terminology being used interchangeably in literature, the authors have agreed upon using the term 'growth ridges' throughout. In *B. hirsutum*, the growth ridges are well developed and hirsute, being covered with numerous chitinous setae projecting outwards from the shell plate, aggregated on small basal domes (Fig. 2H). According to Bourget and Crisp (1975), the rate of ridge formation corresponds roughly to the growth rate of barnacles. However, the ontogenic age of deep-sea species might be affected by the fluctuating food supply in the else stable physical deep-sea environment (Anderson 1994; Foster 1983; Tyler and Young 1992). As generalist feeders, *B. hirsutum* captures suspended particulate matter with help of an erected cirral fan which it is able to adjust towards the prevailing water currents (Southward and Southward 1958; Dayton et al. 1982; Gallego et al. 2017). Adult specimens of *B. hirsutum* can grow more than 8 cm in height and have a white-yellow shell plate colour (Fig. 2A–C, G). The barnacle is of conical shape with the diameter of the orifice being less than half of the diameter of the membranous basis (Newman and Ross 1971; Southward and Southward 1958). Main species-specific characteristics are narrow carinolateral plates, an elongate tergum, and compartments of the orifice which do not diverge from another, as for example seen in *B. corolliforme* (Bullivant & Dearborn, 1967 plate 14; Dayton et al., 1982 fig. 3C; Meyer, 2020 fig. 3–3). The parietal plates of *B. hirsutum* show a wide plasticity, depending on the attachment site as well as the space given for the animal to grow. As many acorn barnacles, *B. hirsutum* is of gregarious nature and tends to settle crowded with epizoic growth, *i.e.*, one established animal having one or several specimens laterally attached (Anderson 1994).

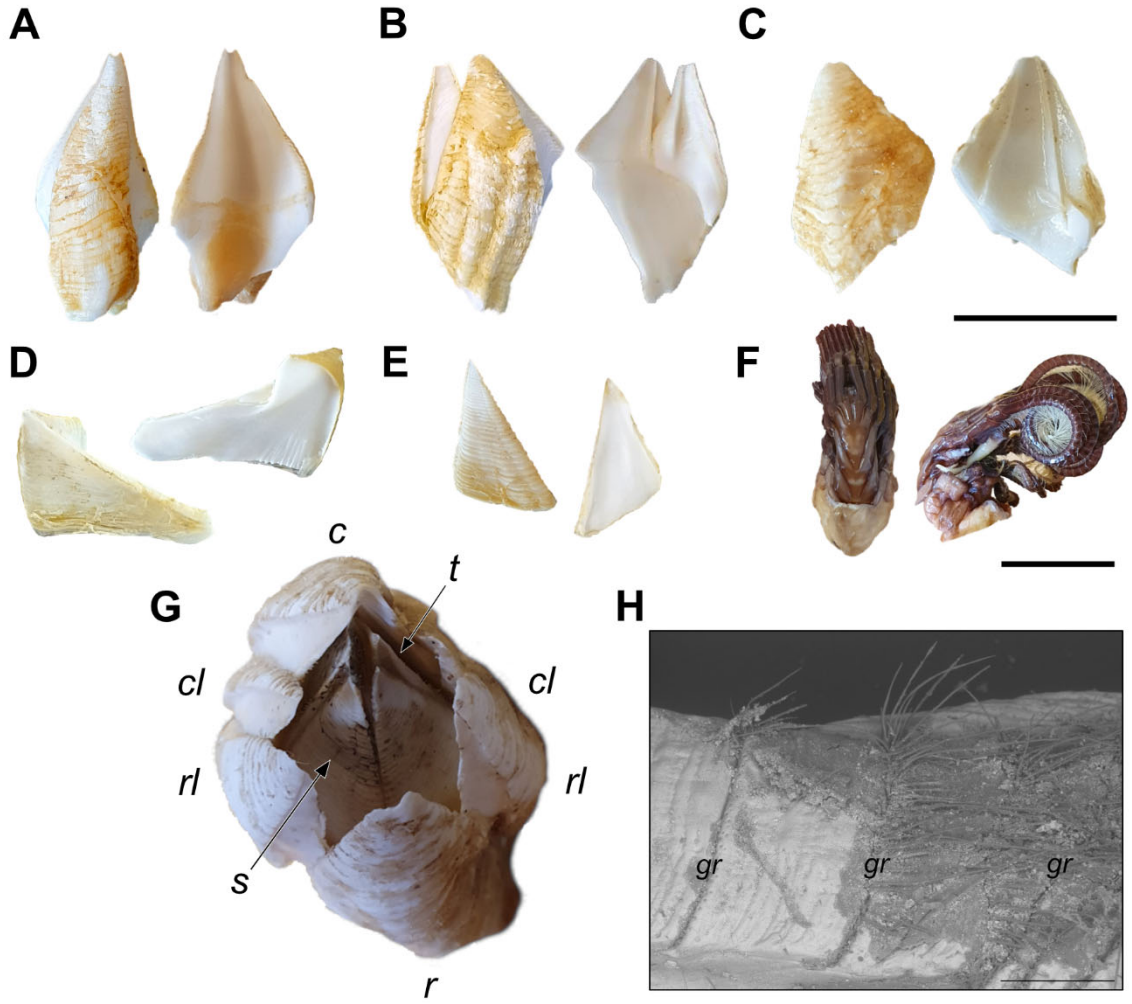

Fig. 2. Plate organisation and general anatomy of *B. hirsutum*. External and internal view of A carina, B rostro-lateral, C rostrum, D tergum, E scutum. F Soft-bodied animal with serrated cirral appendages. G Top view of an intact specimen with a carino-rostral diameter of 2.5 cm; c: carina, cl: carino-lateral, rl: rostro-lateral, r: rostrum, t: tergum, s: scutum. H SEM image of a shell plate showing growth ridges (gr) with protruding chitinous setae. Scale bars: A–C 1.5 cm, D–F 1 cm, H 500 µm.

Scope of study

Processes involving successful recruitment, dispersal of planktotrophic larvae and settlement as benthic animals with future reproductive success determine the extent to which barnacle populations are genetically and biologically connected across their distributional range (Boschen-Rose and Colaço 2021; Cowen et al. 2007; Pineda et al. 2007). As these bentho-pelagic interactions are highly complex and challenging to assess, especially with regard to deep-sea habitats (Etter and Bower 2015), the genetic connectivity of *B. hirsutum* within the NE Atlantic is completely

unknown. In the northeastern Iceland Basin, surface waters of the North Atlantic Current converge with deeper water masses from the Iceland-Faroe Ridge into the East Reykjanes Ridge Current (EERC), acting as a boundary between the Iceland Basin and the eastern flank of the Reykjanes Ridge (Koman et al. 2020). As the broad EERC flows southwest towards the Bight Fracture Zone, it crosses the ridge into the Irminger Basin (Fig. 1). This study reports on the opportunistic inhabitation of a hydrothermally influenced site for the species *B. hirsutum* and elaborates on habitat differences by comparing barnacle size distributions per site and depth, as well as chemical components of parietal shell plates from all sites. Furthermore, we attempt to investigate the genetic connectivity of *B. hirsutum* from four sites within the Iceland Basin, encompassing non-hydrothermal habitats in the Faroe Bank Channel and along the Reykjanes Ridge, as well as the vent-associated habitat. With the ERRC, an oceanographic connectivity pathway to western Atlantic basins, the potential for *B. hirsutum* nauplius larvae to be dispersed across the ridge is elaborated. Given that *B. hirsutum* is herein acknowledged to utilise a hydrothermally influenced habitat, vent fields within its range of depth and occurrence are discussed as potential habitats, as is the potential for *B. corolliforme* and *B. chilense* to live affiliated with hydrothermal activity.

MATERIALS AND METHODS

Taxon sampling and measurements

Specimens of *Bathylasma hirsutum* were collected at four sites (Fig. 3, Table 1) during three research cruises under the IceAGE (Icelandic marine Animals: Genetics and Ecology) project umbrella (Brix and Devey 2019; Brix et al. 2014; Meißner et al. 2018). At site A, situated west of the Faroe Bank Channel, barnacles were sampled by means of a triangular dredge onboard the RV *Poseidon* in 2013 (IceAGE_2 / POS456; Brix et al. 2013). In 2018, specimens were sampled along the Reykjanes Ridge axis at the sites B and C using the Remotely Operated Vehicle (ROV) *Phoca* onboard the RV *Maria S. Merian* (IceAGE_RR / MSM75; Devey et al. 2018). In 2020, the Reykjanes Ridge was revisited with the *RV Sonne* and the ROV *Kiel6000* (IceAGE_3 / SO276; Brix et al. 2020). Barnacles were collected at site D, affiliated with the hydrothermal 'IceAGE vent field' which was discovered during the SO276 expedition (Brix et al. 2020). Prior to and during animal sampling by means of the ROV, each site was documented by *in situ* video and photography records. Material collection was performed using the ROV's operational titanium arms, with nets or the slurp sampler. On deck, specimens were labelled and fixed in sealed plastic bags using 96% undenatured ethanol and stored at -20°C to avoid DNA degeneration. Photographs of each

specimen were taken with a Canon EOS 2000D prior to tissue sampling from the abdomen or one cirrus for DNA analysis. Carina parietal plates were measured by height using a digital vernier calliper, and growth ridges on the carina were counted with the aid of a Leica stereomicroscope. Morphometric measurements of each specimen are listed in the supplementary material (Table S1). Measurements were plotted using R 4.2.2 (R Core Team 2022) and RStudio 7.2.576 (RStudio Team 2022). Respective R packages are listed in the supplementary material (Table S2). Distribution records of *B. hirsutum* were reviewed from original literature and databases (www.jncc.gov.uk, www.gbif.org, www.obis.org) and geographic maps including bathymetric data were created using the software QGIS 3.10 (QGIS Development Team 2019).

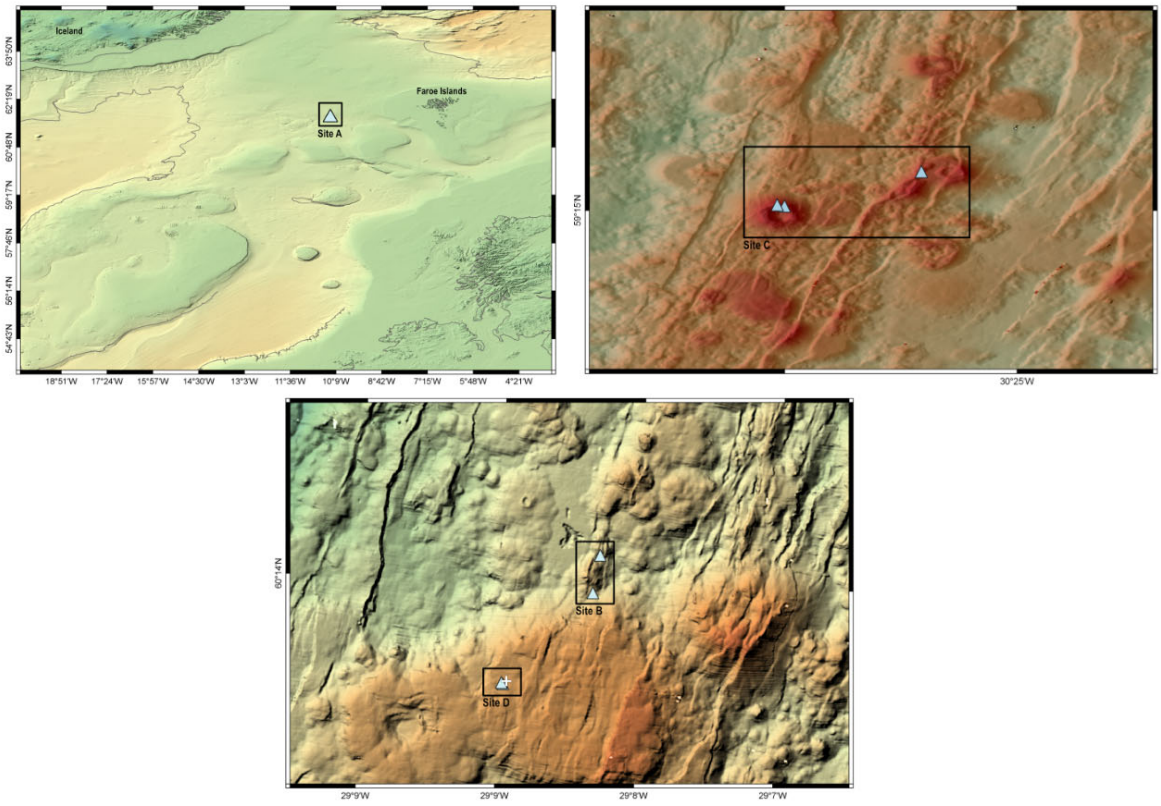

Fig. 3. Collection sites of *Bathylasma hirsutum* targeted during the research cruise POS456 west of the Faroe Bank Channel (site A), as well as two expeditions along the Reykjanes Ridge MSM75 (site B, C), and SO276 (site D). The white cross indicates the hydrothermal IceAGE vent field.

Table 1. Metadata of the four sampling sites A–D. Barnacles of the species *Bathylasma hirsutum* were collected by means of triangular dredge (TD) and remote operated vehicle (ROV)

Expedition	Site	Depth (m)	Latitude 'N	Longitude 'W	Date	Station	Gear
IceAGE_2	A - Faroe Bank Channel	1110	61°44.220	010°19.710	30.07.2013	877	TD
IceAGE_RR	B - Reykjanes Ride	719	60°14.274	029°08.138	07.07.2018	31	ROV
		703	60°14.201	029°08.162	01.08.2018	188	ROV
	C - Reykjanes Ridge	966	59°15.653	030°26.805	17.07.2018	80	ROV
		858 - 867	59°15.074	030°29.102	28.07.2018	149	ROV
IceAGE_3	D - IceAGE vent field	664	60°14.020	029°08.500	12.07.2020	103	ROV
		658	60°14.022	029°08.506	14.07.2020	112	ROV

DNA extraction, amplification and sequencing

DNA extractions were carried out either on board the research vessel or at the research institute. Therefore, three different extraction kits were used; E.Z.N.A® Mollusc DNA Kit (Omega Bio-Tek Inc., Norcross, GA, USA), Qiagen DNeasy® Blood and Tissue Kit (Qiagen, California, USA), and Macherey-Nagel NucleoSpin Tissue Kit (Macherey-Nagel, Düren, Germany); following the manufacturer's instructions, leaving the tissue for digestion overnight in a shaking bath at 56°C/350 rpm. For all isolates, elution was carried out in two steps, using 50 µl elution buffer each turn. DNA concentration for each isolate (100 µl) was measured using a Qubit 4 Fluorometer (Thermo Fischer Scientific™ Inc.), following the manufacturer's protocol. DNA quality was comparable between all extraction methods. All DNA aliquots were stored at -20°C at the German Centre for Marine Biodiversity Research (DZMB), Hamburg. The mitochondrial marker cytochrome *c* oxidase subunit I (*COI*) and the nuclear marker elongation factor 1α subunit (EF-1) were selected for species delimitation analyses (Table 2). Polymerase Chain Reaction (PCR) was carried out using three types of polymerases because of the workflow happening in different laboratories or with regard of troubleshooting. The used polymerases were AccuStart II Taq PCR SuperMix (Quantabio, Beverly, MA, USA), Phire Green Hot Start II PCR Master Mix (Thermo Fischer Scientific™), and PCR-Beads, illustra™ PuReTaq Ready-To-Go™ (Avantor®; VWR Int. GmbH, Darmstadt, Germany). Applied master mix compositions and thermal cycling conditions are listed in the supplementary material (Table S3, S4). Quality and quantity of amplified product was assessed by gel electrophoresis using 1.5 % TAE gels. Where band quantification yielded too high DNA concentration, samples were diluted 1:10 prior to purification. Samples with low DNA content were repeated using the same PCR settings but doubling the amount of amplified DNA. Successful PCR products were purified using 3 µl ExoSAP-IT PCR Product Cleanup Reagent (Thermo Fischer Scientific™) on 10 µl product and run on a thermal cycler (incubation: 37°C, 15 min; enzyme inactivation: 80°C, 15 min). Double stranded sequencing was carried out by the sequencing facilities Macrogen Europe Inc. (Amsterdam, Zuidoost, The Netherlands) and Eurofins Genomics Germany GmbH (Ebersberg, Germany) using ABI 3730xl sequencers.

Table 2. List of primers with annealing temperature (AT) range

Primer	Sequence (5' to 3')	Range of AT (°C)	Reference
COI			
LCO1490	GGTCAACAAATCATAAAGATATTGG	45-50	Folmer et al. 1994
HCO2198	TAAACTTCAGGGTGACCAAAAATCA		
LCO1490-JJ	CHACWAAYCATAAAGATATYGG	55-70	

HCO2198-JJ	AWACTTCVGGRTGVCCAAARAATCA		Astrin and Stüben (2008)
EF-1			
EF-1 for	GATTTCATCAAGAACATGATCAC	56-60	Tsang et al. 2014
EF-1 rev	AGCGGGGGGAAGTCGGTGAA		

Sequence editing, alignment, and genetic analyses

Geneious Prime® (Version 2022.1.1; Biomatters, Auckland, New Zealand; Kearse et al. 2012) was used to edit and assemble forward and reverse chromatograms as well as to check for potential contamination using the implemented BLAST search tool (Basic Local Alignment Search Tool; Altschul et al. 1990). Assembled sequences were aligned using MUSCLE (Edgar 2004), implemented in Geneious Prime® with default settings, and ends trimmed with respective primer sequences. The software jModelTest 2 (Darriba et al. 2012; Guindon and Gascuel 2003) was used to estimate best-fit models of evolution applying the Akaike Information Criterion (AIC; Sakamoto et al. 1986), resulting in GTR + I + G for COI and TIM1 + I + G for EF-1. Phylogenetic analyses of single-gene and concatenated alignments were performed using MrBayes 3.2.1 (Huelsenbeck and Ronquist 2001), with three parallel runs of 5 million generations, sampling every 1000 generations. Convergence of independent runs was examined in Tracer 1.7.2 (Rambaut et al. 2018) with a burn-in of 10 %. Trees were reconstructed using Bayesian Inference (BI), assessing branch support by posterior probability (PP) with values ≥ 0.95 considered as highly supported (Felsenstein 1985; Huelsenbeck et al. 2001). Tree editing was performed in FigTree 1.4.4 (Rambaut 2009) and Affinity Photo 1.10.5 (Serif Ltd., Europe). Species were delimited using the two distance-based methods ASAP (Assemble Species by Automatic Partitioning; Puillandre et al. 2021) and ABGD (Automated Barcode Gap Discovery; Puillandre et al. 2012), using the three evolutionary models Jukes-Cantor; Kimura 80 and Simple Distance with default settings. Haplotype networks were computed for both gene markers using the software PopArt (Leigh and Bryant 2015), applying the minimum spanning network algorithm to calculate nucleotide diversity, Tajima's D test statistic as well as the number of segregating and parsimony-informative sites (Bandelt et al. 1999).

Energy Dispersive Spectroscopy

Energy Dispersive Spectroscopy (EDS) analysis for the elemental presence detection was performed to compare the mineral components of shell plates of *B. hirsutum* from sites with and without hydrothermal influence. EDS was done with a Hitachi TM3000 Scanning Electron

Microscope (Hitachi High-Technologies, Maidenhead, UK), equipped with an Oxford Instrument INCA system and Aztec software (Oxford Instruments, High Wycombe, UK) at the British Antarctic Survey. EDS maps for x150 magnified areas were acquired for five minutes, set to detect all elements, and quantified by the Aztec software. Elemental spectra of the bulk composition (% oxides) were displayed and presence of manganese (Mn), iron (Fe) and rare earth metals (e.g. Tungsten trioxide (WO_3), Ytterbium (III) oxide (Yb_2O_3), Vanadium pentoxide (V_2O_5)) noted.

RESULTS

A total of 159 specimens of *Bathylasma hirsutum* were sampled at four sites (A–D) within the NE Atlantic. Site A extends the northern distributional range of the species from the Wyville Thomson Ridge to the Faroe Bank Channel. Sampling efforts at sites B–D present new records from the central section of Reykjanes Ridge and provide first-time *in situ* observations of the species in its natural habitat (Fig. 4). Video footage of the respective sites can be accessed via the doi:10.5281/zenodo.10220154. The habitat at site B, situated at ~710 m depth, is dominated by large volcanic rocks and pillow lava with varying topography, featuring a range of niches with diverse megafaunal compositions including different species of cold-water corals (Fig. 4A; see also Devey et al. 2018). Barnacle coverage varies from individual specimens along the slope of a volcanic mount to localised patches of high abundance. Active predation by a sea star of unidentified species was observed, next to an empty barnacle shell which likely had been fed upon beforehand. At site C, barnacles occur with highest observed abundances along the northern and western rim of a large, cratered volcano structure between 858 and 966 m depth. At times, debris of dead barnacle shells is found below boulders on which alive adult specimens sit attached (Fig. 4B). Active feeding behaviour by means of complete cirral extension was observed frequently (Fig. 4D). Proximal to the venting chimneys of the recently discovered IceAGE vent field (Brix et al. 2020), barnacles were found attached to volcanic boulders in localised groups, accompanied by several specimens of an orange deep-sea anemone, possibly belonging to the genus *Phelliactis* Simon, 1892 (Fig. 4E, F). During sampling, ambient water temperature was measured to ~5.6°C (see Brix et al. 2020 fig. 5.29). The influence of hydrothermal activity is apparent by the presence of white bacterial mats covering the sea bed. Prior to this study, the settlement of *B. hirsutum* in a hydrothermally influenced habitat had been unacquainted. Of all species of acorn barnacles currently described, *B. hirsutum* represents the first to be found affiliated with a hydrothermal vent field in the Atlantic Ocean.

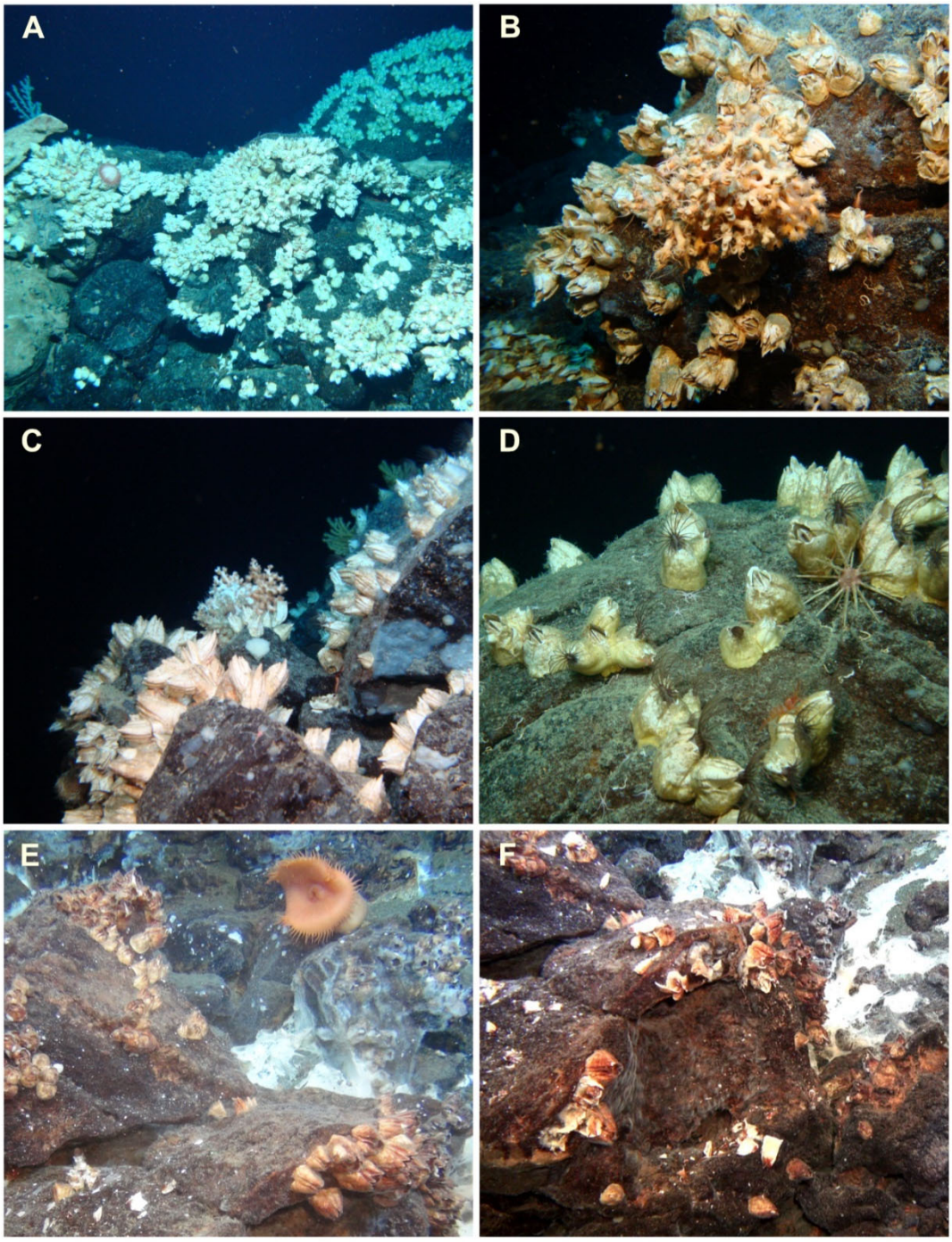

Fig. 4. *In situ* images of *B. hirsutum* from the Reykjanes Ridge axis (A–D) and the IceAGE vent field (E, F). **A** Dense cluster of specimens attached to pillow lava (site B). **B** Barnacles aggregated with a cold-water coral. Accumulated dead shell plates visible to the lower left (site C). **C** Epizoic growth on boulder with associated coral fauna (site C). **D** Feeding behaviour by extended cirral fans in multiple specimens situated on volcanic rock (site C). **E–F** Specimens with brown-black shell precipitate attached to volcanic rocks, surrounded by white bacterial mats (site D). Large orange anemones, possibly of the genus *Phelliactis*, share the habitat. Image courtesy: GEOMAR, Kiel.

Molecular species delimitation

DNA was successfully amplified for 146 specimens, yielding 287 novel sequences for the two genetic markers *COI* (146 sequences; 686 bp) and EF1 (141 sequences; 930 bp). Seventeen sequences were retrieved from GenBank and included in the final analysis. *Chelonibia testudinaria* (Linnaeus, 1758) was used to root trees, as the family Chelonibiidae Pilsbry, 1916 is sister to the Bathylasmatidae (Chan et al. 2021). The Bayesian analyses of the concatenated gene alignment (COI + EF1, 168 sequences; 1616 bp) show maximum support for a single clade of *B. hirsutum* (PP = 1), including specimens from all sampled sites (Fig. 5). The clade clearly separates from the Antarctic sister species *B. corolliforme* (PP = 0.95) as well as from the sister genus *Hexelasma* Hoek, 1913 (P = 1). ABGD and ASAP analyses were run on alignments for both genetic markers. Prior maximum divergence of intraspecific diversity (P) was set to 0.001–0.1 and relative gap width (X) to 1.0–1.5. Each of the evolutionary models yielded a partition consistent with the Bayesian analysis, suggesting one clade of *B. hirsutum* (*P* = 0.00167–0.100). Partitions yielding more than one clade of *B. hirsutum* likely resulted from splitting artefacts caused by the low P values (0.0010; Puillandre et al. 2012, 2021). Sequence data is submitted to GenBank via the BOLD dataset dx.doi.org/10.5883/DS-IACIR. GenBank accession numbers are listed in the supplementary material (Table S5).

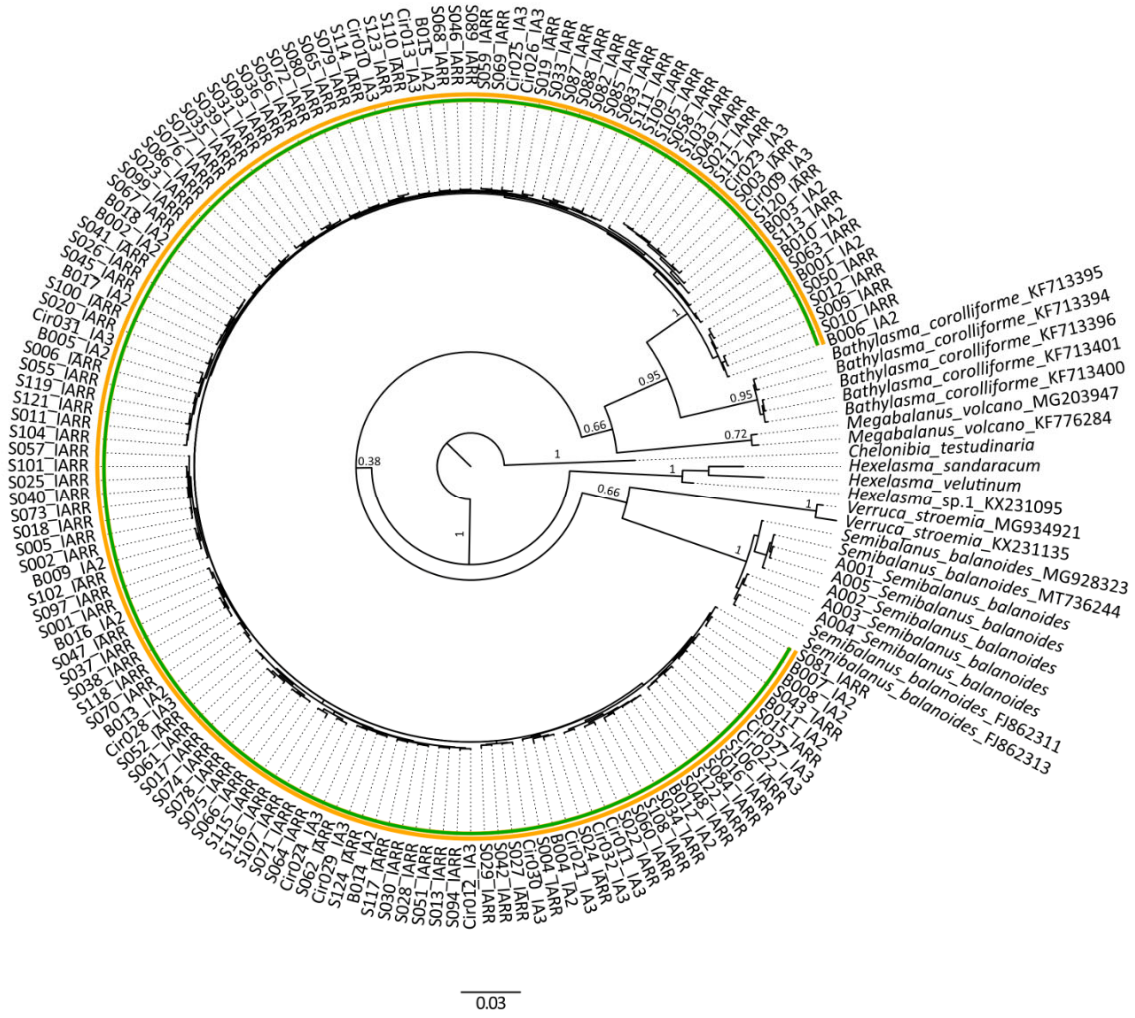

Fig. 5. Bayesian phylogenetic tree with posterior probabilities based on the concatenated COI + EF1 dataset, including seven outgroup species. Names on the nodes refer to the *Bathylasma hirsutum* specimen code and the respective IceAGE expedition. Results of the ASAP and ABGD species delimitations are shown by yellow and green circles. The tree is rooted with *Chelonibia testudinaria*. Scale bar shows substitutions per site.

Haplotype network analyses

Each one minimum-spanning haplotype network was inferred from 146 *COI* and 134 EF1 sequences of *B. hirsutum* to visualise the genetic relationships between individual genotypes at population level (Fig. 6). Both networks depict a high degree of genetic connectivity amongst the sampled sites, reflected in the three (*COI*) and four (EF1) prominent clusters of genetically identical specimens. The genetic distance to smaller clusters or individual samples is low, with a maximum of four mutational steps visualised as hash marks. The low intraspecific genetic diversity is as well reflected in the nucleotide diversity and small number of parsimony-informative sites.

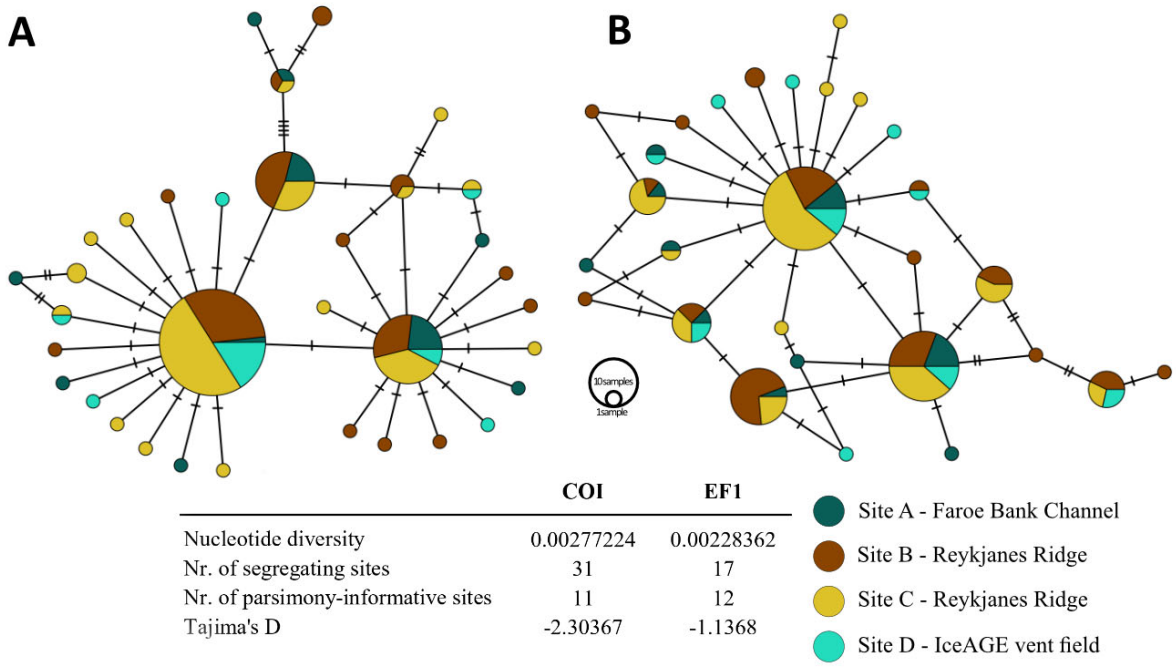

Fig. 6. Minimum spanning haplotype networks and analysis outputs of *Bathylasma hirsutum* from the four sampled sites A–D coded by colour. A, Network of the *COI* sequences. B, Network of the EF1 sequences.

EDS analyses of barnacle plates

Specimens collected at sites A, B, and C depict a natural shell colour, congruent with the morphological species description of *B. hirsutum* (Hoek 1883). Shell plates of specimens from site D, however, are of darkened shade owed to a brown-black shell precipitate (Fig. 4). To examine these extrinsic differences and the composition of the precipitate, elemental spectra of the bulk composition (% oxides) of manganese (Mn), iron (Fe), Tungsten trioxide (WO_3), Ytterbium (III) oxide (Yb_2O_3), and Vanadium pentoxide (V_2O_5) were assessed of selected specimens from each site (Table 3). Shell plates from site D yielded the highest Fe/Mn ratios, with percentages of 2.54–34.82 (FeO) and 1.94–28.59 (MnO) measured from the youngest (base) to the oldest shell part (apex). This results in up to 60.24 % ferromanganese (Fe-Mn), increasing towards the apex. Values of WO_3 double in top and mid sections, whereas Yb_2O_3 is absent. Vanadium pentoxide (V_2O_5) was solely found in the mid-section of one shell plate. Shell plates from sites B and C contained smaller Fe/Mn ratios, yielding traces of Fe-Mn oxide ranging from 0.26–1.35 % and 0.44–1.95 % in the mid-section, to 1.93 % and 2.25 % in the apex, respectively. No ferromanganese oxides were detected in the youngest shell part. Small fractions of WO_3 and Yb_2O_3 are present in the mid sections only. The shell plate from site A yielded 4.56 % FeO in the mid-section, as well as 0.37 % WO_3 in the apex

and 0.64 % Yb_2O_3 at the base. No Fe-Mn oxide precipitates were measured.

Table 3. Energy Dispersive Spectroscopy (EDS) analyses for the elemental presence detection on barnacle plates from stations within the respective sampling areas. Elemental spectra of the bulk composition (% oxides) are shown for the top, mid and end sections of each shell plate with measured presences of iron oxide (FeO), manganese oxide (MnO), ferromanganese oxide (Fe-Mn) and the rare earth metals Tungsten trioxide (WO_3), Ytterbium (III) oxide (Yb_2O_3) and Vanadium pentoxide (V_2O_5). Measurements in the top section of specimen S039 failed and are not accessible (na)

Expedition	Site	Station	Specimen	FeO	MnO	Fe-Mn	WO_3	Yb_2O_3	V_2O_5	Position
IceAGE_2	A	877	B018	0.22 - 0.40	-	-	0.37	-	-	Top
				4.56 - 4.56	-	-	-	-	-	Mid
				0.52 - 9.92	-	-	-	0.64	-	End
IceAGE_RR	B	31	S022	1.13 - 1.19	0.66 - 0.74	1.79 - 1.93	-	-	-	Top
				0.59 - 0.65	0.63 - 0.70	1.22 - 1.35	0.51 - 0.67	-	-	Mid
				0.43 - 0.77	-	-	-	-	-	End
	B	188	S123	0.58 - 0.75	-	-	-			Top
				0.59 - 0.59	0.26 - 0.34	0.36 - 0.93	0.40 - 0.44	0.80	-	Mid
				0.00 - 3.33	-	-	-	-	-	End
	C	80	S039	na	na	na	na	na	na	Top
				0.44 - 0.89	0.00 - 0.15	0.44 - 0.63	0.37	-	-	Mid
				8.85 - 9.05	-	-	-	-	-	End
	C	149	S067	1.58 - 1.67	0.48 - 0.58	2.06 - 2.25	-	-	-	Top
				1.36 - 1.94	0.47 - 0.57	1.83 - 1.95	-	-	-	Mid
				2.18 - 2.22	-	-	-	-	-	End

IceAGE_3	D	103	Cir022	31.56 - 34.82	21.99 - 24.02	53.55 - 58.84	-	-	-	Top
				19.19 - 31.65	28.59 - 16.06	35.25 - 60.24	0.89	-	0.57	Mid
				4.23 - 4.23	2. 87 - 2.87	7.10 - 7.10	-	-	-	End
	D	112	Cir032	15.67 - 16.82	19.81 - 22.42	35.57 - 39.24	1.11	-	-	Top
				11.99 - 15.18	16.41 - 17.48	28.40 - 32.42	1.02 - 1.13	-	-	Mid
				2.54 - 8.05	1.94 - 5.50	4.48 - 13.55	-	-	-	End

Morphometric measurements of carinal shell plates

Intact carinal parietal plates were identified in 69 specimens (site A, B, C, D: 10, 24, 24, 11; see Table S1). Carinal height (CH) was measured from base to apex and plotted against the count of growth ridges (GR) for each parietal plate to map barnacle size distribution per site and visualise the relation between CH and GR (Fig. 7A). Overall, CH has a positive effect on the number of GR, illustrated by the positive slope. The largest CH of 65.48 mm was measured from a site C specimen, with the highest count of 116 GR. The sample set contained the fewest small specimens with a minimum height of 18.53 mm and a count of 28 GR. Barnacles from site A were second largest, with maximum and minimum heights of 29.00 mm and 78.30 mm, and respective counts of 31 and 63 GR. Specimens from site B depicted the largest size span from 5.15 mm to 56.30 mm, with 12 GR and 56 GR laid down on the carinal plates, respectively. Here, the highest GR count of 71 was from a specimen of 44.22 mm carinal plate height. The smallest barnacle from site D sized 14.70 mm and had 12 GR. In the largest specimen of 50.50 mm height, 48 GR were counted. The highest count of 51 was retrieved from a carina sizing 43.20 mm. To test whether barnacle size distribution changes with ocean depth, average depth at each sampled site was plotted against CH (Fig. 7B). Our data denote a trend towards enhanced shell growth at the deeper sites A and C compared to the shallower sites B and D.

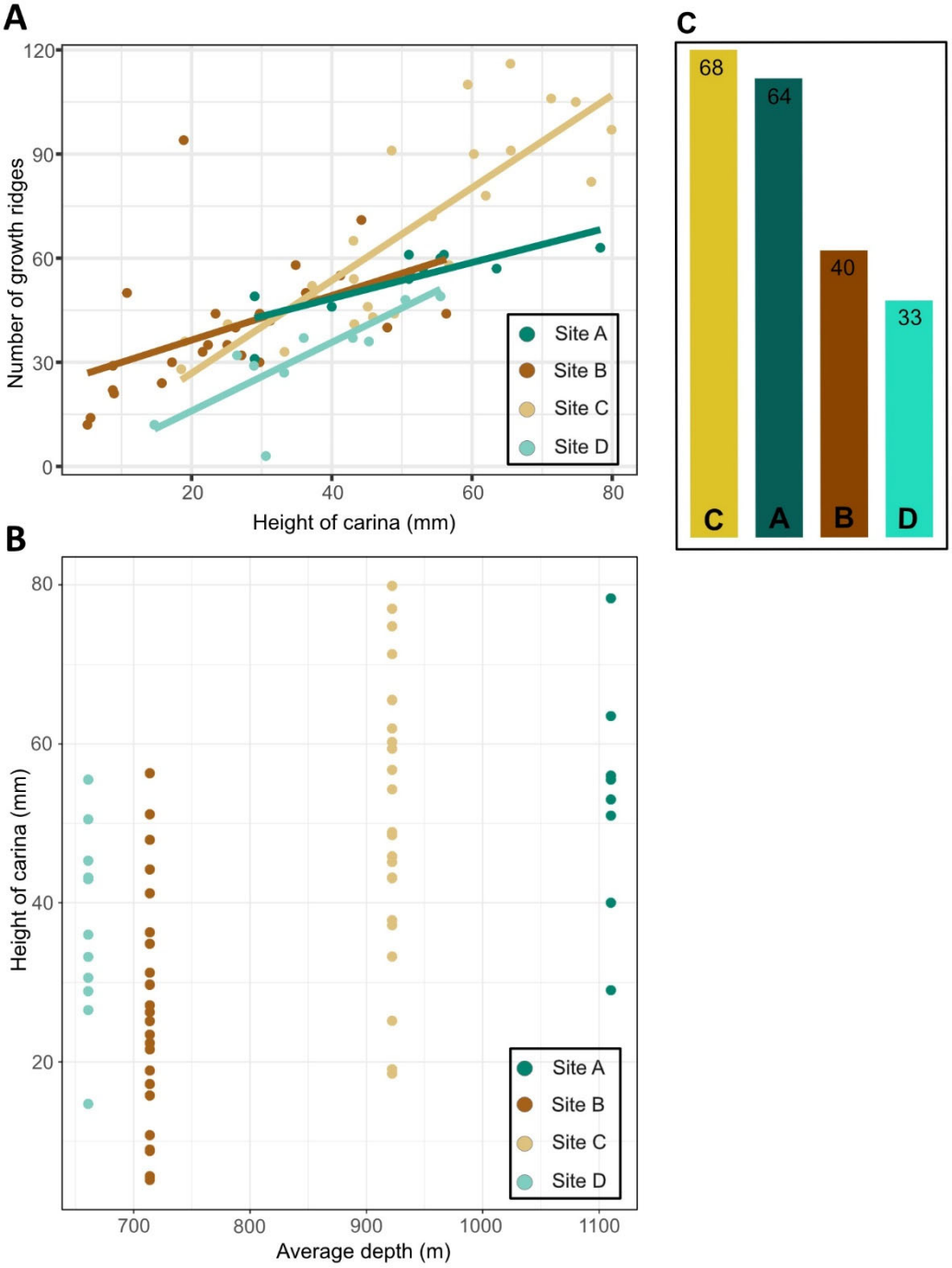

Fig. 7. Morphometric measurements of carinal parietal plates. A, Relation between carinal height and count of growth ridges on the carinal parietal plate with a predicted linear model fits based on a 95% confidence interval. B, Barnacle size distribution represented by carinal height at average depth at the sampled sites. C, Bar chart showing the average number of growth ridges per site.

DISCUSSION

The herein presented results on the deep-sea acorn barnacle *Bathylasma hirsutum* from four sites within the northeastern Iceland Basin provide new distributional records with *in situ* footage of specimens occupying hard-bottom substrates in depths between 658 and 966 meters along the Reykjanes Ridge axis. For the first time, *B. hirsutum* was found affiliated with a hydrothermally active field. As it is unknown to which extent populations of this sessile crustacean with planktotrophic larval dispersal are connected, we have assessed the genetic connectivity between specimens from the Faroe Bank Channel and the Reykjanes Ridge. The molecular analyses revealed low levels of intraspecific genetic diversity, reflected in the low number of parsimony-informative sites. Latter indicate the observed intraspecific genetic variability to be lower than the expected genetic variation between specimens of *B. hirsutum* from different sites (Papathanassopoulou and Lorentzos 2014). Haplotype networks of both markers suggest a substantial gene flow between all sites (Fig. 6), indicating a pronounced genetic connectivity within the Iceland Basin. Site A, situated west of the Faroe Bank Channel, now marks the northern boundary of the species' distributional range. Based on the basin-wide cluster analysis conducted by Schumacher et al. (2022), this site is categorised as nutrient-rich, with strong local currents and seasonal changes. It is highly hydrodynamic, influenced by the continuous flow of dense, well-oxygenated Iceland Scotland Overflow Water (Chafik et al. 2020; Hansen et al. 2016) with mean water temperatures at maximum depth between 4–9°C (Assis et al. 2018; Tyberghein et al. 2012). The hard-bottom habitat houses several dense aggregations of benthic suspension feeding organisms such as sponges and cold-water coral reefs, indicating a prominent food supply (Frederiksen et al. 1992; Kazanidis et al. 2019). Strong current velocities do not only enhance particle suspension and thus food supply, making this a favourable habitat for *B. hirsutum*, but may also provide pathways for larval transport. As the deep-water currents interconnect with water flows along the eastern flank of the Reykjanes Ridge, we suggest a proportion of larvae dispersed from site A to be transported towards the Reykjanes Ridge axis, facilitating the high localised abundances observed during the ROV dives (Fig. 4A). The ridge axis is mainly influenced by the ERRC, a weakly bottom-intensified current resulting from a convergence of dense Iceland Scotland Overflow Water with the Iceland branch of the North Atlantic Current (Koman et al. 2020). With these nutrient-rich and well-oxygenated water masses flowing south, larvae are suggested to be transported along the ridge, facilitating the genetic connectivity between the herein assessed sites. We presume that recruits of *B. hirsutum* settled at site D originated from the dense barnacle fields north of this site. With ambient seawater temperatures measured to ~5.6°C where the vent-affiliated specimens were sampled (see Devey et al. 2018), the habitat suitability by means of temperature range is comparable to the non-hydrothermally influenced sites.

Analysis of morphometric measurements

The positive relation between carinal plate heights and number of growth ridges laid down on the respective shell plates reflects the formation of growth ridges to be a good indication for the growth rate of the deep-sea barnacle *B. hirsutum*, such as it is for shallow-water species (Bourget and Crisp 1975). In what way the number of growth ridges can be related to the age of a specimen, however, seems to be depth-dependent. In an experimental study on growth ridge formation, Bourget and Crisp (1975) observed one growth ridge to be laid down for each one exuviation in the intertidal species *S. balanoides*, reflecting an annual growth pattern. In the deep-sea species *B. corolliforme*, however, the authors counted many more ridges than the observed number of moults and were not able to distinguish between the ridges laid down on the shell during and in absence of a moulting event. Hence, in *B. corolliforme*, one growth ridge cannot be estimated to account for one year, but rather a growth period which in turn is affected by food availability. The principal food source in deep-sea habitats is owed to vertical flux of organic matter from both surface primary production and redistribution of suspended particles in the bottom mixed layers (Davies et al. 2009, 2006; Ramirez-Llodra et al. 2010). With *B. hirsutum* being sister to the Antarctic *B. corolliforme* and occupying habitats with comparable physical environments, we suggest a similar pattern of growth ridge formation in this species where a fluctuating food supply in the else stable physical deep-sea environment might affect the growth rate (Anderson 1994; Foster 1983; Tyler and Young 1992).

Carinal parietal plates from the two deeper sites A and C were found to be larger compared to the shallower habitats at site B and D, implying barnacle size to be greater with increased depth (Fig. 7). This trend is congruent with the general understanding of deep-sea species to grow larger with depth, adapted to invest already restricted energy resources in growth (Timofeev 2001). At site C, specimens were found in highest abundance and are not only largest but also show the highest amount of growth periods. We suggest the high abundances and enhanced growth at the volcanic crater to be a response to an enriched food environment accompanied by strong localised currents, providing a favourable habitat for *B. hirsutum*. The productive food environment is also reflected in a massive coral forest, dominated by large trees of *Paragorgia arborea* (Linnaeus, 1758), which was detected proximal to the barnacle fields (Devey et al. 2018). This is further supported by the frequently sighted active feeding behaviour (Fig. 4D). The accumulated shell debris observed below several boulders with alive specimens still attached indicates a long-sustained population with several generations of settlement. The large size span of individuals collected at site B indicates a vital population with successful recruitment of juveniles, settled amongst their adult conspecifics (Fig. 7A). Since several specimens sizing less than 10 mm in carinal height were found, food

availability in this habitat is assumed to be slightly lower compared to site C, yielding a lowered individual growth rate. At the hydrothermally-influenced site D, specimens were found to be smaller compared to the deeper sites (Fig. 7C). This is interesting, as *B. hirsutum* could potentially utilise matter from the widespread bacterial mats as an additional food source. This mixotroph mode has been confirmed in several stalked barnacle species from hydrothermal vent fields in the Pacific Ocean (Buckeridge 2000; Southward and Newman 1998) and was recently suggested for the acorn barnacle genus *Eochionelasmus* (Chan et al. 2020). If *B. hirsutum* were adapted to this feeding mode, we would expect to find barnacles of similar or even increased size which is not mirrored in our observations (Fig. 7). Accounting for that the species rather opportunistically utilises the hard-rock substrate in vicinity of the vent field and does not live directly associated with the hydrothermally active chimneys, we assume that *B. hirsutum* is not adapted to integrate organic matter from bacterial mats. In addition to the smaller size range, less growth ridges were counted on carinal parietal plates that were of comparable height to specimens from non-hydrothermally influenced sites (Fig. 7A). These results imply that growth ridge formation might be impacted by the pronounced shell precipitate, possibly eroding the ridges in the process of the accumulation of ferromanganese oxides. Overall, our results imply barnacle shell size to increase with ocean depth (Fig. 7B). However, this snapshot of barnacle size distribution requires more detailed attention to verify whether this trend applies across the entire distributional range of the species.

Ferromanganese oxide shell precipitates

The formation of iron (Fe), manganese (Mn) and ferromanganese (Fe-Mn) mineral deposits happens by migration of Fe and Mn cations from less oxidising to more oxidising conditions (Glasby 2006; Park et al. 2023). Marine Fe-Mn deposits may form as crusts, nodules or are contained within layers of rock and are classified by three mineralisation types; hydrogenetic, diagenetic, and hydrothermal (Marino et al. 2019; Usui et al. 2020). Hydrogenetic Fe-Mn crust deposits form by precipitation of Fe oxyhydroxide and Mn oxide from ambient seawater onto the bedrock on i.e. continental shelves and seamounts (Lusty et al. 2018). Hydrothermal processes, on the other hand, lead to the accumulation of Fe-Mn oxides from plume discharge (Connelly et al. 2007; Muiños et al. 2013; Sujith and Gonsalves 2021). At the Reykjanes Ridge, plume discharge from the Steinahóll vent field contains a high concentration of dissolvable manganese (~60 nmol/l; Taylor et al. 2021). Equivalent discharge is expected to occur at the IceAGE vent field, situated ~400 km south on the same volcanic ridge axis. Inactive ridges such as the Iceland-Faroe Ridge do not display such enrichments (Horowitz 1974). Since there are no records of hydrothermal activity in the vicinity of site A, it is plausible that the chemical component analysis yielded no traces of

ferromanganese (Table 3). None of the specimens from site B, despite being situated just ~450 m north of the IceAGE hydrothermal vent field, were observed with shell precipitate. In accordance with the circulation patterns and bottom currents prevailing along the eastern flank of the Reykjanes Ridge, the plume discharge by the IceAGE vent field is likely to be carried in a south-western direction relative to the active chimneys (Horowitz 1974; Koman et al. 2020; Ruddiman 1972). Hence, Fe-Mn traces from hydrothermal origin seem not to reach barnacles from site B. Situated south of the vent field, specimens collected at site C could be in range to be affected by plume discharge. However, throughout the distance of ~130 km, trace elements such as Fe and Mn are likely to have been accreted to sediments or precipitated as crust deposits in the proximate environment before reaching the barnacle field (Connelly et al. 2007; Horowitz 1974). The minor percentage of Fe-Mn oxide measured in shells from both sites (Table 3) is rather contemplated to reference to ambient water Mn and Fe concentrations as barnacles show a strong affinity for incorporating both Fe and Mn into their shells compared to other calcifying animals (Pilkey and Harriss 1966; Ullmann et al. 2018). Merely specimens at site D had pronounced Fe-Mn precipitates on their parietal plates, visible as dark brown-black deposits from the apex to the base. The high Fe/Mn ratios reflect an enrichment from hydrothermal plume discharge emanated from the IceAGE vent field. Detailed geochemical analyses on the enrichment of trace elements in the hydrothermal plume are desirable to assess whether the Fe-Mn enrichment could additionally be a product of diagenetic processes. In this case, high contents of typical diagenetic elements such as Ni, Cu and Co would need to be present (Schiellerup et al. 2021). In general, shell plates from site D contained a higher percentage of rare earth metal components compared to sites A–C, especially with regard of Tungsten trioxide. This is coherent, as this metal has been found to accumulate in ferromanganese deposits (Kunzendorf and Glasby 1992).

Previous to our study, the affiliation of *B. hirsutum* with hydrothermal vent systems was unacquainted. Still, the presence of shell precipitates has not gone fully unnoticed. During a geological survey, intact barnacles were collected together with coral fragments at 800 m depth on the Reykjanes Ridge, at a station situated central between the herein sampled sites B and C (Murton et al. 1995). Without further commenting on a possible source of origin, the authors reported a manganese staining on the barnacles, which were later identified as *B. hirsutum* by Copley et al. (1996), who however omitted to mention the precipitate. The reported manganese staining is likely to be Fe-Mn oxide and could have originated from plume discharge emanated from site D, or even from another yet undetected hydrothermal source in this area. On the Azores Archipelago, Southward (1998) examined several hundred dead shell plates of *B. hirsutum* collected together with dead pieces of *Desmophyllum pertusum* (Linnaeus, 1758) between 1250 and 1630 m depth. Both barnacles and corals were described to depict a black manganese coating. As the collected

material had died off, we assume that the precipitate formed through either hydrogenous or diagenetic sources, as for example observed in shark teeth or coral skeletons (Edinger and Sherwood 2012; Iyer 1999). Based on the high amount of barnacle shells, Southward (1998) estimated that the sampled area must had been densely populated by *B. hirsutum* in earlier times and suggested a possible enrichment from hydrothermal sources which would have enabled the high abundance of specimens. The Lucky Strike vent field, situated ~12 km west of this area and described just shortly before (Langmuir et al. 1997), could be considered as a potential hydrothermal source of enrichment. However, the once high abundance of *B. hirsutum* could also have sustained due to strong prevailing currents that transport nutrient-rich, well-oxygenated water masses along the MAR (Puerta et al. 2020; Fig. 1). With regard to our observations of a rather low abundance of *B. hirsutum* at the IceAGE vent field (Fig. 4E, F), the transport of nutrients by ocean currents is regarded to have a much higher impact on barnacle abundance compared to the influence of hydrothermal activity. If latter were to be the main source, the abundance of *B. hirsutum* ought to have been much greater than what we observed at site D.

On the affiliation of *Bathylasma* with hydrothermally influenced habitats

This study acknowledges the habitat ambient to the IceAGE vent field as a suitable living space for *B. hirsutum*. As the recognised maximum depth for *B. hirsutum* is 1829 m, NE Atlantic hydrothermal vent fields deeper than 2000 m are anticipated to be out of the species' ecological range for successful settlement in these habitats. Within its known depth range, however, several records from the MAR spreading centre on the Azores Archipelago overlap with recognised hydrothermal active sites (Beaulieu and Szafrański 2020). Given from west to east, *B. hirsutum* has been recorded ~800 m off Ribeira Quente (Young 1998), and Don Joao de Castro Bank (Gruvel 1920), ~784 m south of Espalamaca (Young 1998), ~860 m south of LUSO (Poltarukha and Zevina 2006a), and ~12 km west of the Lucky Strike vent field (Southward 1998). Repeated sampling efforts by means of a ROV are highly encouraged to investigate whether *B. hirsutum* in fact is affiliated with the recognised hydrothermal active fields and whether the barnacles utilise these habitats in a comparable fashion to what has been observed at the IceAGE vent field, including observations on possible shell precipitates.

Detailed biological surveys of the myriad hydrothermal systems in the world oceans are a major task still (Tunnicliffe et al. 2003; Van Dover et al. 2006). We hypothesise that future research activities on hydrothermal vent systems within the distributional range of the bathylasmatid sister species *Bathylasma corolliforme* and *Bathylasma chilense* will reveal their potential to utilise hydrothermally influenced habitats, in a comparable manner to what has been found for *B. hirsutum*

in this study. As for the sister species *B. corolliforme*, Dayton et al. (1982) reported specimens from 400 m depth attached to volcanic rocks. The sampling locality is situated south of the Pacific-Antarctic Ridge. In this region, hydrothermal activity has been inferred from several localities (Beaulieu and Szafrański 2020; Bell et al. 2016; Linse et al. 2022; Rogers et al. 2012; Tao et al. 2012) and distal hydrothermal influences have been suggested (Sieber et al. 2021) within the given depth range of the species. Furthermore, a high abundance of unidentified deep-sea acorn barnacles was detected on an active volcanic mount structure at 2221 m depth during the Marion Rise Expedition programme (Koepke et al. 2020). However not mentioned in the respective cruise report, publicly available video footage documents this observation from the Marion Rise (marumTV 2020; 43°53.6822'S 39°13.3234'E). We believe these barnacles to belong to the species *B. corolliforme* as species-specific characters such as the strong diverging orifical compartments are clearly visible (see Bullivant and Dearborn 1967 plate 14; Dayton et al. 1982 fig. 3C; Meyer 2020 fig. 3-3) and the observations were captured from a site west of the species' type locality (Hoek 1883). Unfortunately, no material was sampled and examined in further detail during the Marion Rise expedition.

Just recently, the sister species *B. chilense* was described based on three specimens collected from 1800–2000 m depth off Caldera, northern Chile (Araya and Newman 2018). The type locality is situated in vicinity of the Peru-Chile Trench, an area of subduction and earthquake activity. As the vast majority of seafloor venting in the southern hemisphere remains unexplored still, the number of hydrothermal vent sites on this actively spreading ridge may be many to discover (Baker et al. 2016; Beaulieu and Szafrański 2020). In line with further deep-sea explorations off the Chilean coast, we hypothesise *B. chilense* to be found affiliated with hydrothermal activity, utilising these habitats in a comparative manner to what has been presented here for *B. hirsutum* from the NE Atlantic.

A connectivity pathway to the northwest Atlantic?

By date, no records of *B. hirsutum* are known from any of the north-western (NW) Atlantic basins. There is, however, one fossil record of the extinct sister species *B. corrugatum* from the continental shelf break off North Carolina, indicating that these bathylasmatid acorn barnacles managed to sustain at least one population in the NW Atlantic during the Neogene and Paleogene periods (Zullo and Baum 1979). In fact, the westward flow of the East Reykjanes Ride Current merging with the Irminger Current could serve as a connectivity pathway into the Irminger Basin as well as the David Strait, facilitating larval distribution of *B. hirsutum* to suitable hard-bottom habitats along the shelf breaks. Such habitats were recently surveyed by Kenchington et al. (2017)

who discovered a reef of *Desmophyllum pertusum* at 886–932 m depth on a steep slope in the Davis Strait. The herein reported temperature range of 4.13–5.03°C as well as current velocities of 10-15 cm s^{-1} could indeed facilitate an eligible habitat for barnacle recruits and already established, actively feeding individuals (see Southward and Southward 1958). Increased sampling efforts in NW Atlantic basins and along the continental shelf breaks could possibly reveal yet undiscovered occurrences of *B. hirsutum*. Special focus ought to be given to the coastline off America as the type of *Hexelasma americanum* Pilsbry, 1916, a species of sister genus to *Bathylasma*, was sampled here (Pilsbry 1916). Showing high morphological similarity and occupying overlapping habitats on the Azores Archipelago (Poltarukha and Zevina 2006a; Young 1998 2001), we suggest that both species require similar environmental conditions to sustain vital populations. Hence, it might be possible that a co-existence of *Bathylasma* and *Hexelasma* along the western Atlantic shelf is present, but has been left unrecognised due to their morphological similarities (Newman and Ross 1971; Southward and Southward 1958).

CONCLUSIONS

The Reykjanes Ridge provides a variety of hard-bottom habitats which are dominated by saline, nutrient-rich and well oxygenated water masses as well as strong current regimes (Puerta et al. 2020; Schumacher et al. 2022). Much effort is still needed to understand the extent and functions of biological communities found in these habitats, with special regard to hydrothermally influenced sites. Our investigations on the deep-sea acorn barnacle *B. hirsutum* contribute to a better understanding of the benthic sessile fauna with planktotrophic larval dispersal and related connectivity patterns in the North Atlantic. Our molecular sampling approach has not only extended the genetic dataset of this species, but aided to investigate the genetic connectivity between four sampled sites in the northeastern Iceland Basin. The comprehensive literature review on the species revealed a high number of sampling records as well as a series of detailed studies on favourable habitats in this species. However, previous to this study, *in situ* footage of these large invertebrates remained absent, as did the acknowledgement of hydrothermally influenced habitats as a suitable living space. Our findings of small local abundances on volcanic rocks in vicinity of the IceAGE vent field do not only extend the knowledge on a favourable habitat, but also emphasise the need for further research that is ought to be focused on the Reykjanes Ridge axis, as well as on hydrothermal habitats shallower than 1800 meters along the extensive Mid-Atlantic Ridge.

List of abbreviations

MAR, Mid-Atlantic Ridge.
PP, Posterior Probability.
BI, Bayesian Inference.
ASAP, Assemble Species by Automatic Partitioning.
ABGD, Automated Barcode Gap Discovery.
EDS, Energy Dispersive Spectroscopy.
BOLD, Barcode Of Life Database.
CH, Carinal height.
GR, Growth ridge.

Acknowledgments: The authors are grateful for the funding support by the German Science Foundation (IceAGE_2: grant BR3843/4-1; IceAGE_RR: grant BR3843/5-1; IceAGE_3: grant MerMet17-06) and the Bundesministerium für Bildung und Forschung (SO276). We like to thank the crew, chief scientists and scientific staff of *RV Poseidon* during IceAGE_2 (POS456), *RV Maria S. Merian* during IceAGE_RR (MSM75), and *RV Sonne* during IceAGE_3 (SO276). A special thanks to Antje Fischer (TA DZMB Hamburg), Karen Jeskulke (TA DZMB Hamburg), and Nicole Gatzemeier (TA DZMB Hamburg) for their support in sample logistics, Dr. Nancy Mercado Salas and Angelina Eichsteller for their support with the molecular analyses, Mia Schumacher (GEOMAR, Kiel) for her support with the bathymetry and map compilations, and the ROV team from GEOMAR for their contributions to collect specimens and obtain high quality video and image material. This study is a contribution to the EU Horizon 2020 iAtlantic project. The funders had no role in study design, data collection and analysis, decision to publish, or preparation of the manuscript.

Authors' contributions: Sample collections were conducted by SB and PMA during IceAGE_2, by SB, KL and JT during IceAGE_RR, and by JN, SB and JT during IceAGE_3. KL and JT conceived the study and conducted initial morphometric measurements. KL performed the SEM imaging and EDS scanning. PMA aided with data analyses guidance. JN performed the study, analysed the specimen data and the imagery/video data, prepared figures and tables, authored or reviewed drafts of the paper and compiled all data and manuscript pieces. All authors read and approved the final manuscript.

Competing interests: All authors declare that they have no competing interests.

Availability of data and materials: Metadata, genetic data and specimen images are deposited in the Barcode Of Life Database (BOLD) and accessible via the doi: dx.doi.org/10.5883/DS-IACIR. Novel COI and EF1 sequences are submitted to the NCBI GenBank and available by the accession numbers OQ026012–OQ026166. *The authors are currently depositing video material with publicly accessible DOIs to Zenodo. These will be listed upon final submission.*

Consent for publication: All authors consent to the publication of this manuscript.

Ethics approval consent to participate: Not applicable. The species is not under the listed categories of experimental animals that need ethics approval.

REFERENCES

Aldred N, Alsaab A, Clare AS. 2018. Quantitative analysis of the complete larval settlement process confirms Crisp's model of surface selectivity by barnacles. Proc R Soc B Biol Sci **285:**1–9. doi:10.1098/rspb.2017.1957.

Altschul SF, Gish W, Miller W, Myers EW, Lipman DJ. 1990. Basic Local Alignment Search Tool. J Mol Biol **215:**403–410. doi:10.1016/S0022-2836(05)80360-2.

Anderson DT. 1994. Barnacles. Structure, Function, Development and Evolution. Chapman & Hall, London.

Araya JF, Newman WA. 2018. A new deep-sea balanomorph barnacle (Cirripedia: Thoracica: Bathylasmatidae) from Chile. PLoS ONE **13:**1–15. doi:10.1371/journal.pone.0197821.

Assis J, Tyberghein L, Bosch S, Verbruggen H, Serrão EA, De Clerck O. 2018. Bio-ORACLE v2.0: Extending marine data layers for bioclimatic modelling. Glob Ecol Biogeogr **27:**277–284. doi:10.1111/geb.12693.

Astrin JJ, Stüben PE. 2008. Phylogeny in cryptic weevils: Molecules, morphology and new genera of western Palaearctic Cryptorhynchinae (Coleoptera: Curculionidae). Invertebr Syst **22:**503–522. doi:10.1071/IS07057.

Baker ET, Resing JA, Haymon RM, Tunnicliffe V, Lavelle JW, Martinez F, Ferrini V, Walker SL, Nakamura K. 2016. How many vent fields? New estimates of vent field populations on ocean ridges from precise mapping of hydrothermal discharge locations. Earth Planet Sci Lett **449:**186–196. doi:10.1016/j.epsl.2016.05.031.

Bandelt HJ, Forster P, Röhl A. 1999. Median-joining networks for inferring intraspecific

phylogenies. Mol Biol Evol **16:**37–48. doi:10.1093/oxfordjournals.molbev.a026036.

Barnes H, Barnes M. 1959. Some parameters of growth in the common intertidal barnacle, *Balanus balanoides* (L.). J Mar Biol Assoc United Kingdom **38:**581–587.

Barnes H, Barnes M. 1958. The Rate of Development of *Balanus balanoides* (L.) Larvae. Limnol Oceanogr **3**:29–32.

Beaulieu SE, Szafrański KM. 2020. InterRidge Global Database of Active Submarine Hydrothermal Vent Fields Version 3.4. PANGAEA. doi:10.1594/PANGAEA.917894.

Bell JB, Woulds C, Brown LE, Sweeting CJ, Reid WDK, Little CTS, Glover AG. 2016. Macrofaunal Ecology of Sedimented Hydrothermal Vents in the Bransfield Strait, Antarctica. Front Mar Sci **3:**1–15. doi:10.3389/fmars.2016.00032.

Bielecki J, Chan BKK, Høeg JT, Sari A. 2009. Antennular sensory organs in cyprids of balanomorphan cirripedes: Standardizing terminology using *Megabalanus rosa*. Biofouling **25:**203–214. doi: 10.1080/08927010802688087.

Biscoito M, Almeida AJ, Segonzac M. 2006. Preliminary biological characterization of the Saldanha hydrothermal field at the Mid-Atlantic Ridge (36°34′N, 32°26′W, 2200 m). Cah Biol Mar **47:**421–427.

Blomsterberg M, Glenner H, Høeg JT. 2004. Growth and Molting in Epizoic Pedunculate Barnacles Genus *Octolasmis* (Crustacea: Thecostraca: Cirripedia: Thoracica). J Morphol **260:**154–164. doi:10.1002/jmor.10132.

Boschen-Rose RE, Colaço A. 2021. Northern Mid-Atlantic Ridge Hydrothermal Habitats: A Systematic Review of Knowledge Status for Environmental Management. Front Mar Sci **8:**1–23. doi:10.3389/fmars.2021.657358.

Bourget E. 1987. Barnacle shells: Composition, structure, and growth. *In*: Southward AJ (ed) Barnacle Biology. A.A.Balkema, Rotterdam, pp. 267–285.

Bourget E, Crisp DJ. 1975. An analysis of the growth bands and ridges of barnacle shell plates. J Mar Biol Assoc United Kingdom **55:**439–461. doi:10.1017/S0025315400016052.

Brix S, Cannon J, Svavarsson J, Eilertsen M, Kenning M, Schnurr S, Jennings R, Hoffmann S, Jeskulke K, Holst S, Martínez Arbizu P. 2013. Icelandic marine Animals: Genetics and Ecology Cruise Report POS456 IceAGE2. doi:10.3289/CR.

Brix S, Devey CW. 2019. Stationlist of the IceAGE project (Icelandic marine Animals Genetics and Ecology) expeditions. Mar Data Arch. doi:10.14284/349.

Brix S, Meißner K, Stransky B, Halanych KM, Jennings RM, Kocot KM, Svavarsson J. 2014. The IceAGE project - A follow up of BIOICE. Polish Polar Res **35:**141–150. doi:10.2478/popore-2014-0010.

Brix S, Taylor J, Le Saout M, Mercado-Salas NF, Kaiser S, Lörz A-N, Gatzemeier N, Jeskulke K,

Kürzel K, Neuhaus J, Paulus E, Uhlir C, Korfhage S, Bruhn M, Stein T, Wilsenack M, Siegler V, … Suck I. 2020. Depth transects and connectivity along gradients in the North Atlantic and Nordic Seas in the frame of the IceAGE project (Icelandic marine Animals: Genetics and Ecology). Cruise No. SO276 (MerMet17-06). eprint/58300/1/SO276_Cruise_Report.

Buckeridge JS. 2000. *Neolepas osheai* sp. nov., a new deep-sea vent barnacle (Cirripedia: Pedunculata) from the Brothers Caldera, south-west Pacific Ocean. New Zeal J Mar Freshw Res **34:**409–418. doi:10.1080/00288330.2000.9516944.

Buhl-Mortensen L, Høeg JT. 2006. Reproduction and larval development in three scalpellid barnacles, *Scalpellum scalpellum* (Linnaeus 1767), *Ornatoscalpellum stroemii* (M. Sars 1859) and *Arcoscalpellum michelottianum* (Seguenza 1876), Crustacea: Cirripedia: Thoracica): Implications for repro. Mar Biol **149:**829–844. doi: 10.1007/s00227-006-0263-y.

Bullivant JS, Dearborn JH. 1967. The fauna of the Ross Sea. Part 5. General accounts, station lists, and benthic ecology. New Zeal Dep Sci Ind Res Bull **176:**1–77.

Chafik L, Hátún H, Kjellsson J, Larsen KMH, Rossby T, Berx B. 2020. Discovery of an unrecognized pathway carrying overflow waters toward the Faroe Bank Channel. Nat Commun **11:**1–10. doi:10.1038/s41467-020-17426-8.

Chan BKK, Dreyer N, Gale AS, Glenner H, Ewers-Saucedo C, Pérez-Losada M, Kolbasov GA, Crandall KA, Høeg JT. 2021. The evolutionary diversity of barnacles, with an updated classification of fossil and living forms. Zool J Linn Soc **193:**789–846. doi:10.1093/zoolinnean/zlaa160.

Chan BKK, Ju SJ, Kim DS, Kim SJ. 2020. First discovery of the sessile barnacle *Eochionelasmus* (Cirripedia: Balanomorpha) from a hydrothermal vent field in the Indian Ocean. J Mar Biol Assoc United Kingdom **100:**585–593. doi:10.1017/S0025315420000466.

Checa AG, Salas C, Rodríguez-Navarro AB, Grenier C, Lagos NA. 2019. Articulation and growth of skeletal elements in balanid barnacles (Balanidae, Balanomorpha, Cirripedia). R Soc Open Sci **6:**1–20. doi:10.1098/rsos.190458.

Connelly DP, German CR, Asada M, Okino K, Egorov A, Naganuma T, Pimenov N, Cherkashev G, Tamaki K. 2007. Hydrothermal activity on the ultra-slow spreading southern Knipovich Ridge. Geochemistry, Geophys Geosystems **8:**1–11. doi:10.1029/2007GC001652.

Copley JTP, Tyler PA, Sheader M, Murton BJ, German CR. 1996. Megafauna from sublittoral to abyssal depths along the Mid-Atlantic ridge south of Iceland. Oceanol Acta **19:**549–559.

Cowen RK, Gawarkiewicz G, Pineda J, Thorrold SR, Werner FE. 2007. Population Connectivity in Marine Systems An Overview. Oceanography **20:**14–21.

Cravo A, Foster P, Almeida C, Company R, Cosson RP, Bebianno MJ. 2007. Metals in the shell of *Bathymodiolus azoricus* from a hydrothermal vent site on the Mid-Atlantic Ridge. Environ Int

33:609–615. doi:10.1016/j.envint.2007.01.002.

Crisp DJ. 1955. The behaviour of barnacle cyprids in relation to water movement over a surface. Jorunal Exp Biol **32:**569–590.

Darriba D, Taboada GL, Doallo R, Posada D. 2012. jModelTest2: more models, new heuristics and parallel computing. Nat Methods **9:**772.

Davies AJ, Duineveld GCA, Lavaleye MSS, Bergman MJN, Van Haren H, Roberts JM. 2009. Downwelling and deep-water bottom currents as food supply mechanisms to the cold-water coral *Lophelia pertusa* (Scleractinia) at the Mingulay Reef complex. Limnol Oceanogr **54:**620–629. doi:10.4319/lo.2009.54.2.0620.

Davies AJ, Narayanaswamy BE, Hughes DJ, Roberts JM. 2006. An Introduction to the Benthic Ecology of the Rockall - Hatton Area (SEA 7). A Report for the DTI by the Scottish Association for Marine Science, Dunstaffnage Marine Laboratory, Oban.

Dayton PK, Newman WA, Oliver J. 1982. The Vertical Zonation of the Deep-Sea Antarctic Acorn Barnacle, *Bathylasma corolliforme* (Hoek): Experimental Transplants from the Shelf Into Shallow Water. J Biogeogr **9:**95–109. doi:10.2307/2844695.

Desbruyéres D, Almeida A, Biscoto M, Comtet T, Khripounoff A, Le Bris N, Sarradin PM, Segonzac M. 2000. A review of the distribution of hydrothermal vent communities along the northern Mid-Atlantic Ridge: Dispersal vs. environmental controls. Hydrobiologia **440:**201–2016. doi:10.1023/A:1004175211848.

Desbruyères D, Segonzac M, Bright M. 2006. Handbook of Deep-Sea Hydrothermal Vent Fauna. Biologiezentrum der Oberösterreichische Landesmuseen, Linz, Austria.

Devey C, Brix S, Barua AR, Bodendorfer M, Cuno P, Frutos I, Huusmann H, Kurbjuhn T, Le Saout M, Linse K, Matthiessen T. 2018. Detailed Mapping and Sampling of the Reykjanes Ridge, Cruise No. MSM75, 29 June 2018 - 8 August 2018, Reykjavik-Reykjavik. doi:10.48433/cr_msm75.

DiBacco C, Fuchs HL, Pineda J, Helfrich K. 2011. Swimming behavior and velocities of barnacle cyprids in a downwelling flume. Mar Ecol Prog Ser **433:**131–148. doi:10.3354/meps09186.

Duineveld GCA, Lavaleye MSS, Bergman MJN, De Stigter H, Mienis F. 2007. Trophic structure of a cold-water coral mound community (Rockall Bank, NE Atlantic) in relation to the near-bottom particle supply and current regime. Bull Mar Sci **81:**449–467.

Duperron S, Bergin C, Zielinski F, Blazejak A, Pernthaler A, McKiness ZP, DeChaine E, Cavanaugh CM, Dubilier N. 2006. A dual symbiosis shared by two mussel species, *Bathymodiolus azoricus* and *Bathymodiolus puteoserpentis* (Bivalvia: Mytilidae), from hydrothermal vents along the northern Mid-Atlantic Ridge. Environ Microbiol **8:**1441–1447. doi:10.1111/j.1462-2920.2006.01038.x.

Edgar RC. 2004. MUSCLE: multiple sequence alignment with high accuracy and high throughput. Nucleic Acids Res **32:**1792–7. doi:10.1093/nar/gkh340.

Edinger EN, Sherwood OA. 2012. Applied taphonomy of gorgonian and antipatharian corals in Atlantic Canada: Experimental decay rates, field observations, and implications for assessing fisheries damage to deep-sea coral habitats. Neues Jahrb fur Geol und Palaontologie - Abhandlungen **265:**199–218. doi:10.1127/0077-7749/2012/0255.

Etter RJ, Bower AS. 2015. Dispersal and population connectivity in the deep North Atlantic estimated from physical transport processes. Deep Res Part I Oceanogr Res Pap **104:**159–172. doi:10.1016/j.dsr.2015.06.009.

Fabri MC, Bargain A, Briand P, Gebruk A, Fouquet Y, Morineaux M, Desbruyeres D. 2011. The hydrothermal vent community of a new deep-sea field, Ashadze-1, 12°58′N on the Mid-Atlantic Ridge. J Mar Biol Assoc United Kingdom **91:**1–13. doi: 10.1017/S0025315410000731.

Fautin DG, Barber BR. 1999. *Maractis rimicarivora*, a new genus and species of sea anemone (Cnidaria: Anthozoa: Actinaria: Actinostolidae) from an Atlantic hydrothermal vent. Proc Biol Soc Washingt **112:**624–631.

Felsenstein J. 1985. Confidence Limits on Phylogenies: An Approach Using the Bootstrap. Evolution. **39:**783–791. doi:10.2307/2408678.

Folmer O, Black M, Hoeh W, Lutz R, Vrijenhoek R. 1994. DNA primers for amplification of mitochondrial cytochrome c oxidase subunit I from diverse metazoan invertebrates. Mol Mar Biol Biotechnol **3:**294–299. doi:10.1071/ZO9660275.

Foster BA. 1989. Balanomorph Barnacle Larvae in the Plankton at McMurdo Sound, Antarctica. Polar Biol **10:**175–177. doi: 10.1007/BF00238492.

Foster BA. 1983. Complemental males in the barnacle *Bathylasma alearum* (Cirripedia: Pachylasmidae). *In*: Lowry JK (ed) Papers from the Conference on the Biology and Evolution of Crustacea, Australian Museum Memoir Vol. 18. ,The Australian Museum, Sydney, New South Wales. pp. 133–139.

Foster BA. 1978. The Marine Fauna of New Zealand: Barnacles (Cirripedia: Thoracica). New Zealand Oceanographic Insitute Memoir, Wellington.

Foster BA, Buckeridge JS. 1995. Barnacles (Cirripedia: Thoracica) of seas off the Straits of Gibraltar. Bull du Muséum Natl d'histoire Nat **17:**163–192.

Frederiksen R, Jensen A, Westerberg H. 1992. The distribution of the scleractinian coral *Lophelia pertusa* around the Faroe Islands and the relation to internal tidal mixing. Sarsia **77:**157–171. doi:10.1080/00364827.1992.10413502.

Gage JD. 1986. The benthic fauna of the Rockall Trough: regional distribution and bathymetric

zonation. Proc R Soc Edinburgh Sect B Biol Sci **88:**159–174. doi:10.1017/s026972700000453x.

Gage JD, Tyler PA. 1991. Deep-Sea Biology: A Natural History of Organisms at the Deep-Sea Floor. Cambridge University Press, Cambridge.

Gallego R, Dennis TE, Basher Z, Lavery S, Sewell MA. 2017. On the need to consider multiphasic sensitivity of marine organisms to climate change: a case study of the Antarctic acorn barnacle. J Biogeogr **44:**2165–2175. doi:10.1111/jbi.13023.

Gebruk A V., Budaeva NE, King NJ. 2010. Bathyal benthic fauna of the Mid-Atlantic Ridge between the Azores and the Reykjanes Ridge. J Mar Biol Assoc United Kingdom **90:**1–14. doi:10.1017/S0025315409991111.

Gebruk A V., Galkin S V., Vereshchaka AL, Moskalev LI, Southward AJ. 1997. Ecology and Biogeography of the Hydrothermal Vent Fauna of the Mid-Atlantic Ridge. Adv Mar Biol **32:**93–144. doi:10.1016/s0065-2881(08)60016-4.

German CR, Briem J, Chin C, Danielsen M, Holland S, James R, Jónsdóttir A, Ludford E, Moser C, Ólafsson J, Palmer MR, Rudnicki MD. 1994. Hydrothermal activity on the Reykjanes Ridge: the Steinahóll vent-field at 63°06′N. Earth Planet Sci Lett **121:**647–654. doi:10.1016/0012-821X(94)90098-1.

Glasby GP. 2006. Manganese: predominant role of nodules and crusts. *In*: Schulz HD and Zabel M (eds). Marine Geochemistry. Springer, Heidelberg. pp. 371–427.

Gruvel A. 1920. Cirrhipèdes provenant des Campagnes Scientifiques de S.A.S. le Prince de Monaco (1885-1931). Résultats des Campagnes Sci Accompl sur son Yacht par Albert 1er **53:**3–88.

Gruvel A. 1903. Révision des Cirrhipédes Operculés. I. Partie Systematique. *In*: Nouvelles Archives du Muséum d'Histoire Naturelle. Vol. 5. Masson, Paris, pp. 95–170.

Guindon S, Gascuel O. 2003. A simple, fast and accurate method to estimate large phylogenies by maximum-likelihood. Syst Biol **52:**696–704.

Hansen B, Husgaro KM, Hátún H, Østerhus S. 2016. A stable Faroe Bank Channel overflow 1995-2015. Ocean Sci **12:**1205–1220. doi:10.5194/os-12-1205-2016.

Herrera S, Watanabe H, Shank TM. 2015. Evolutionary and biogeographical patterns of barnacles from deep-sea hydrothermal vents. Mol Ecol **24:**673–689. doi:10.1111/mec.13054.

Hoek PPC. 1883. Report on the Cirripedia collected by the H.M.S. "Challenger" during the years 1873–1876. Rep Sci Results Voyag HMS "Challenger" (1873-76), Zoology, **25:**1–169.

Høeg JT, Møller OS. 2006. When similar beginnings lead to different ends: Constraints and diversity in cirripede larval development. Invertebr Reprod Dev **49:**125–142. doi:10.1080/07924259.2006.9652204.

Horowitz A. 1974. The geochemistry of sediments from the northern Reykjanes Ridge and the

Iceland-Faroes Ridge. Mar Geol **17:**103–122. doi:10.1016/0025-3227(74)90051-6.

Huelsenbeck JP, Ronquist F. 2001. MRBAYES: Bayesian inference of phylogenetic trees. Bioinformatics **17:**754–755.

Huelsenbeck JP, Ronquist F, Nielsen R, Bollback JP. 2001. Bayesian Inference of Phylogeny and Its Impact on Evolutionary Biology. Science **294:**2310–2314. doi:10.1126/science.1065889.

Iyer SD. 1999. Ferromanganese oxides on sharks' teeth from Central Indian Ocean Basin. Indian J Mar Sci **28:**263–269.

Jones DS. 2000. Crustacea Cirripedia Thoracica: Chionelasmatoidea and Pachylasmatoidea (Balanomorpha) of New Caledonia, Vanuatu and Wallis and Futuna Islands, with a review of all currently assigned taxa. *In*: Crosnier A (ed). Résultats des Campagnes MUSORSTOM, Volume 21. Memoires du Muséum National d'Histoire Naturelle Vol. 184. Paris. pp. 141–283.

Kazanidis G, Vad J, Henry LA, Neat F, Berx B, Georgoulas K, Roberts JM. 2019. Distribution of Deep-Sea Sponge Aggregations in an Area of Multisectoral Activities and Changing Oceanic Conditions. Front Mar Sci **6:**1–15. doi:10.3389/fmars.2019.00163.

Kearse M, Moir R, Wilson A, Stones-Havas S, Cheung M, Sturrock S, Buxton S, Cooper A, Markowitz S, Duran C, Thierer T, Ashton B, Meintjes P, Drummond A. 2012. Geneious Basic: An integrated and extendable desktop software platform for the organization and analysis of sequence data. Bioinformatics **28:**1647–1649. doi:10.1093/bioinformatics/bts199.

Keeton JA, Searle RC, Parsons B, White RS, Murton BJ, Parson LM, Peirce C, Sinha MC. 1997. Bathymetry of the Reykjanes Ridge. Mar Geophys Res **19:**55–64. doi:10.1023/A:1004266721393.

Kenchington E, Yashayaev I, Tendal OS, Jørgensbye H. 2017. Water mass characteristics and associated fauna of a recently discovered *Lophelia pertusa* (Scleractinia: Anthozoa) reef in Greenlandic waters. Polar Biol **40:**321–337. doi:10.1007/s00300-016-1957-3.

Koepke J, Beier C, Dick HJB, Achten A, Albers E, Becker H, Böhnke M, Bongartz T, Brunelli D, Cheadle M, Codillo E, Engelhardt A, Genske FS, Hanisch M, Hansen C, Klar S, Klein F, … Zhou Z. 2020. ROV-Sampling and Mapping of the Marion Rises at the Southwest Indian Ridge (SWIR), Cruise No. SO273, 06.03.2020 - 22.04.2020, Cape Town (South Africa) - Emden (Germany). doi:10.2312/cr_so273.

Koman G, Johns WE, Houk A. 2020. Transport and Evolution of the East Reykjanes Ridge Current. J Geophys Res **125:**1–18. doi:10.1029/2020JC016377.

Kongsrud JA, Budaeva N, Barnich R, Oug E, Bakken T. 2013. Benthic polychaetes from the northern Mid-Atlantic Ridge between the Azores and the Reykjanes Ridge. Mar Biol Res **9**:516–546. doi:10.1080/17451000.2012.749997.

Kunzendorf H, Glasby GP. 1992. Tungsten accumulation in Pacific ferromanganese deposits. Miner

Depos **27:**147–152. doi:10.1007/BF00197100.

Lagersson NC, Høeg JT. 2002. Settlement behavior and antennulary biomechanics in cypris larvae of *Balanus amphitrite* (Crustacea: Thecostraca: Cirripedia). Mar Biol **141:**513–526. doi:10.1007/s00227-002-0854-1.

Langmuir C, Humphris S, Fornari D, Van Dover C, Von Damm K, Tivey MK, Colodner D, Charlou JL, Desonie D, Wilson C, Fouquet Y, Klinkhammer G, Bougault H. 1997. Hydrothermal vents near a mantle hot spot: The Lucky Strike vent field at 37°N on the Mid-Atlantic Ridge. Earth Planet Sci Lett **148:**69–91. doi:10.1016/s0012-821x(97)00027-7.

Leigh JW, Bryant D. 2015. POPART: Full-feature software for haplotype network construction. Methods Ecol Evol **6:**1110–1116. doi:10.1111/2041-210X.12410.

Linse K, Römer M, Little CTS, Marcon Y, Bohrmann G. 2022. Megabenthos habitats influenced by nearby hydrothermal activity on the Sandwich Plate, Southern Ocean. Deep Res Part II Top Stud Oceanogr **198:**1–13. doi:10.1016/j.dsr2.2022.105075.

López-González PJ, Rodríguez E, Gili JM, Segonzac M. 2003. New records on sea anemones (Anthozoa: Actiniaria) from hydrothermal vents and cold seeps. Zool Verh **345:**215–243.

Lusty PA, Hein JR, Josso P. 2018. Formation and Occurrence of Ferromanganese Crusts: Earth's Storehouse for Critical Metals. Elements **14:**313–318.

Marino E, González FJ, Kuhn T, Madureira P, Wegorzewski A V., Mirao J, Medialdea T, Oeser M, Miguel C, Reyes J, Somoza L, Lunar R. 2019. Hydrogenetic, Diagenetic and Hydrothermal Processes Forming Ferromanganese Crusts in the Canary Island Seamounts and Their Influence in the Metal Recovery Rate with Hydrometallurgical Methods. Minerals **9:**1–42. doi:10.3390/min9070439.

Maruzzo D, Aldred N, Clare AS, Høeg JT. 2012. Metamorphosis in the cirripede Crustacean Balanus amphitrite. PLoS ON **7:**1–8. doi: 10.1371/journal.pone.0037408.

marumTV 2020. Expedition SO273 "Marion Rise": Deep Sea Video Highlights. [Video]. YouTube. https://www.youtube.com/watch?v=PAGh3WrDpyk.

Meißner K, Brix S, Halanych KM, Jażdżewska AM. 2018. Preface – biodiversity of Icelandic waters. Mar Biodivers **48:**715–718. doi:10.1007/s12526-018-0884-7.

Meyer N. 2020. Polar microbioerosion patterns exemplified in Arctic and Antarctic barnacles. PhD Dissertation, University of Bremen, Germany.

Meyer N, Wisshak M, Freiwald A. 2021. Bioerosion ichnodiversity in barnacles from the Ross Sea, Antarctica. Polar Biol **44:**667–682. doi:10.1007/s00300-021-02825-4.

Muiños SB, Hein JR, Frank M, Monteiro JH, Gaspar L, Conrad T, Pereira HG, Abrantes F. 2013. Deep-sea Fe-Mn Crusts from the Northeast Atlantic Ocean: Composition and Resource Considerations. Mar Georesources Geotechnol **31:**40–70.

doi:10.1080/1064119X.2012.661215.

Murton BJ, Parson L, Evans J, Owens R, Satur N, Redbourn L, Sauter D, Taylor R, Walker CL, Forster J, Anderson J, Fern A, Jones J, Paulson C, Phipps R, Wyner J. 1995. RSS Charles Darwin Cruise CD80, 01 Sep-01 Oct 1993. The PETROS Programme (PETRogenesis of Oblique Spreading). Cruise Report No. 241.

Narayanaswamy BE, Howell KL, Hughes DJ, Davies JS, Roberts JM, Black KD. 2006. Strategic Environmental Assessment Area 7 Photographic Analysis Report. Department of Trade and Industry, London, United Kingdom.

Narayanaswamy BE, Hughes DJ, Howell KL, Davies J, Jacobs C. 2013. First observations of megafaunal communities inhabiting George Bligh Bank, Northeast Atlantic. Deep Res II **92:**79–86. doi:10.1016/j.dsr2.2013.03.004.

Newman WA, Ross A. 1971. Antarctic Cirripedia. Antarct Res Ser **14:**1–257.

Ó Foighil D, Jennings R, Park J-K, Merriwether DA. 2001. Phylogenetic relationships of mid-oceanic ridge and continental lineages of *Lasaea* spp. (Mollusca: Bivalvia) in the northeastern Atlantic. Mar Ecol Prog Ser **213:**165–175. doi:10.3354/meps213165.

Papathanassopoulou AD, Lorentzos NA. 2014. Parsimony-Informative Characters. *In*: 9th Conf. Hellenic Society for Computational Biology and Bioinformatics. pp. 10–12.

Park K, Jung J, Park J, Ko Y, Lee Y, Yang K. 2023. Geochemical-mineralogical analysis of ferromanganese oxide precipitated on porifera in the Magellan seamount, western Pacific. Front Mar Sci **9:**1–11. doi:10.3389/fmars.2022.1086610.

Pérez-Losada M, Høeg JT, Simon-Blecher N, Achituv Y, Jones D, Crandall KA. 2014. Molecular phylogeny, systematics and morphological evolution of the acorn barnacles (Thoracica: Sessilia: Balanomorpha). Mol Phylogenet Evol **81:**147–158. doi:10.1016/j.ympev.2014.09.013.

Pilkey OH, Harriss RC. 1966. The effect of intertidal environment on the composition of calcareous skeletal material. Limnol Oceanogr **11:**381–385.

Pilsbry HA. 1916. The Sessile Barnacles (Cirripedia) Contained in the Collections of the U.S. National Museum; Including a Monograph of the American Species. Bull United States Natl Museum **93:**1–366.

Pineda J, Hare JA, Sponaugle S. 2007. Larval Transport and Dispersal in the Coastal Ocean and Consequences for Population Connectivity. Oceanography **20**:22–39. doi:10.5670/oceanog.2007.27.

Pineda MO, Gebauer P, Briceño FA, López BA, Paschke K. 2021. A bioenergetic approach for a novel aquaculture species, the giant barnacle *Austromegabalanus psittacus* (Molina, 1788): Effects of microalgal diets on larval development and metabolism. Aquac Reports **21:**1–14.

doi:10.1016/j.aqrep.2021.100824.

Pineda J, Riebensahm D, Medeiros-Bergen D. 2002. *Semibalanus balanoides* in winter and spring: Larval concentration, settlement, and substrate occupancy. Mar Biol **140:**789–800. doi:10.1007/s00227-001-0751-z.

Poltarukha OP, Zevina GB. 2006a. Barnacles (Cirripedia, Thoracica) of the north-eastern Atlantic. *In*: Mironov AN, Gebruk AV and Southward AJ (eds). Biogeography of the North Atlantic seamounts. KMK Scientific Press, Moscow, Russia. pp. 162–176.

Poltarukha OP, Zevina GB. 2006b. Barnacles (Cirripedia, Thoracica) of the Reykjanes Ridge. *In*: Mironov AN, Gebruk AV and Southward AJ (eds). Biogeography of the North Atlantic seamounts. KMK Scientific Press, Moscow, Russia. pp. 152–161.

Puerta P, Johnson C, Carreiro-Silva M, Henry LA, Kenchington E, Morato T, Kazanidis G, Rueda JL, Urra J, Ross S, Wei CL, González-Irusta JM, Arnaud-Haond S, Orejas C. 2020. Influence of Water Masses on the Biodiversity and Biogeography of Deep-Sea Benthic Ecosystems in the North Atlantic. Front Mar Sci **7:**1–25. doi:10.3389/fmars.2020.00239.

Puillandre N, Brouillet S, Achaz G. 2021. ASAP: assemble species by automatic partitioning. Mol Ecol Resour **21:**609–620. doi:10.1111/1755-0998.13281. Available at: https://bioinfo.mnhn.fr/abi/public/asap/asapweb.html

Puillandre N, Lambert A, Brouillet S, Achaz G. 2012. ABGD, Automatic Barcode Gap Discovery for primary species delimitation. Mol Ecol **21:**1864–1877. doi:10.1111/j.1365-294X.2011.05239.x. Available at: https://bioinfo.mnhn.fr/abi/public/abgd/abgdweb.html

Rambaut A. 2009. FigTree: Tree figure drawing tool. http://tree.bio.ed.ac.uk/software/figtree/

Rambaut A, Drummond AJ, Xie D, Baele G, Suchard MA. 2018. Posterior summarisation in Bayesian phylogenetics using Tracer 1.6. Syst Biol **67:**901–904. doi:10.1093/sysbio/syy032.

Ramirez-Llodra E, Brandt A, Danovaro R, De Mol B, Escobar E, German CR, Levin LA, Martinez Arbizu P, Menot L, Buhl-Mortensen P, Narayanaswamy BE, Smith CR, Tittensor DP, Tyler PA, Vanreusel A, Vecchione M. 2010. Deep, diverse and definitely different: Unique attributes of the world's largest ecosystem. Biogeosciences **7:**2851–2899. doi:10.5194/bg-7-2851-2010.

Rogers AD, Tyler PA, Connelly DP, Copley JT, James R, Larter RD, Linse K, Mills RA, Garabato AN, Pancost RD, Pearce DA, Polunin NVC, German CR, Shank T, Boersch-Supan PH, Alker BJ, Aquilina A, … Zwirglmaier K. 2012. The Discovery of New Deep-Sea Hydrothermal Vent Communities in the Southern Ocean and Implications for Biogeography. PLoS Biol **10:**1–17. doi:10.1371/journal.pbio.1001234.

Ruddiman WF. 1972. Sediment Redistribution on the Reykjanes Ridge: Seismic Evidence. Geol Soc Am Bull **83:**2039–2062.

Sakamoto Y, Ishiguro M, Kitagawa G. 1986. Akaike Information Criterion Statistics. D. Reidel,

Dordrecht, The Netherlands. p. 290.

Schiellerup H, Ferreira P, González FJ, Marino E, Somoza L, Medialdea T. 2021. Deliverable 3.3: Metallogeny of hydrothermal deposits in European waters. GeoERA-MINDeSEA project. Geological Survey of Norway (NGU), Trondheim, Norway. p. 66.

Schumacher M, Huvenne VAI, Devey CW, Arbizu PM, Biastoch A, Meinecke S. 2022. The Atlantic Ocean landscape: A basin-wide cluster analysis of the Atlantic near seafloor environment. Front Mar Sci **9:**1–17. doi:10.3389/fmars.2022.936095.

Searle RC, Keeton JA, Owens RB, White RS, Mecklenburgh R, Parsons B, Lee SM. 1998. The Reykjanes Ridge: structure and tectonics of a hot-spot-influenced, slow-spreading ridge, from multibeam bathymetry, gravity and magnetic investigations. Earth Planet Sci Lett **160:**463–478. doi:10.1016/S0012-821X(98)00104-6.

Shields MA, Blanco-Perez R. 2013. Polychaete abundance, biomass and diversity patterns at the Mid-Atlantic Ridge, North Atlantic Ocean. Deep Res Part II Top Stud Oceanogr **98:**315–325. doi:10.1016/j.dsr2.2013.04.010.

Sieber M, Conway TM, de Souza GF, Hassler CS, Ellwood MJ, Vance D. 2021. Isotopic fingerprinting of biogeochemical processes and iron sources in the iron-limited surface Southern Ocean. Earth Planet Sci Lett **567:**1–12. doi:10.1016/j.epsl.2021.116967.

Sigvaldadóttir E, Desbruyères D. 2003. Two new species of Spionidae (Annelida: Polychaeta) from Mid-Atlantic Ridge hydrothermal vents. Cah Biol Mar **44:**219–225.

Southward AJ. 1998. New Observations on Barnacles (Crustacea: Cirripedia) of the Azores Region. Arquipélago Life Mar Sci **16A:**11–27.

Southward AJ, Jones DS. 2003. A Revision of Stalked Barnacles (Cirripedia: Thoracica: Scalpellomorpha: Eolepadidae: Neolepadinae) Associated with Hydrothermalism, Including a Description of a New Genus and Species from a Volcanic Seamount off Papua New Guinea. Senckenberg marit **32:**77–93. doi: 10.1007/BF03043086.

Southward AJ, Newman WA. 1998. Ectosymbiosis between filamentous sulphur bacteria and a stalked barnacle (Scalpellomorpha, Neolepadinae) from the Lau Back Arc Basin, Tonga. Cah Biol Mar **39:**259–262.

Southward AJ, Southward EC. 1958. On the occurrence and behaviour of two little-known barnacles, *Hexelasma hirsutum* and *Verruca recta*, from the continental slope. J Mar Biol Assoc United Kingdom **37:**633–647. doi:10.1017/S0025315400005683.

Sujith PP, Gonsalves MJBD. 2021. Ferromanganese oxide deposits: Geochemical and microbiological perspectives of interactions of cobalt and nickel. Ore Geol Rev **139:**1–16. doi:10.1016/j.oregeorev.2021.104458.

Tao C, Lin J, Guo S, Chen YJ, Wu G, Han X, German CR, Yoerger DR, Zhou N, Li H, Su X, Zhu

J. 2012. First active hydrothermal vents on an ultraslow-spreading center: Southwest Indian Ridge. Geology **40:**47–50. doi:10.1130/G32389.1.

Taylor J, Devey C, Le Saout M, Petersen S, Kwasnitschka T, Frutos I, Linse K, Lörz AN, Pałgan D, Tandberg AH, Svavarsson J, Thorhallsson D, Tomkowicz A, Egilsdóttir H, Ragnarsson S, Renz J, Markhaseva EL, … Brix S. 2021. The Discovery and Preliminary Geological and Faunal Descriptions of Three New Steinahóll Vent Sites, Reykjanes Ridge, Iceland. Front Mar Sci **8:**1–20. doi:10.3389/fmars.2021.520713.

Thiyagarajan V, Harder T, Qian P-Y. 2002. Relationship between cyprid energy reserves and metamorphosis in the barnacle *Balanus amphitrite* Darwin (Cirripedia; Thoracica). J Exp Mar Bio Ecol **280:**79–93. doi: 10.1016/S0022-0981(02)00415-X.

Tsang LM, Chu KH, Nozawa Y, Chan BKK. 2014. Morphological and host specificity evolution in coral symbiont barnacles (Balanomorpha: Pyrgomatidae) inferred from a multi-locus phylogeny. Mol Phylogenet Evol **77:**11–22. doi:10.1016/j.ympev.2014.03.002.

QGIS Development Team 2019. QGIS Geographic Information System. *In*: Open Source Geospatial Foundation Project.

R Core Team 2022. R: A language and environment for statistical computing. R Foundation for Statistical Computing. Vienna, Austria. https://www.R-project.org/.

RStudio Team. 2022. RStudio: Integrated Development Environment for R. RStudio, PBC, Boston, MA. http://www.rstudio.com/.

Timofeev SF. 2001. Bergmann's Principle and Deep-Water Gigantism in Marine Crustaceans. Biol Bull **28:**646–650.

Tunnicliffe V, Baross JA, Gebruk AV, Giere O, Holland ME, Koschinsky A, Reysenbach A-L, Shank TM. 2003. Group Report: What are the interactions between biotic processes at vents and physical, chemical and geological conditions? *In*: Halback PE, Tunnicliffe V and Hein JR (eds). Energy and Mass Transfer in Marine Hydrothermal Systems. Dahlem Press, Berlin, Germany, pp. 251–270.

Tyberghein L, Verbruggen H, Pauly K, Troupin C, Mineur F, De Clerck O. 2012. Bio-ORACLE: A global environmental dataset for marine species distribution modelling. Glob Ecol Biogeogr **21:**272–281. doi:10.1111/j.1466-8238.2011.00656.x.

Tyler PA, Young CM. 1992. Reproduction in marine invertebrates in "stable" environments: The deep sea model. Invertebr Reprod Dev **22:**185–192. doi:10.1080/07924259.1992.9672271.

Ullmann C V., Gale AS, Huggett J, Wray D, Frei R, Korte C, Broom-Fendley S, Littler K, Hesselbo SP. 2018. The geochemistry of modern calcareous barnacle shells and applications for palaeoenvironmental studies. Geochim Cosmochim Acta **243:**149–168. doi:10.1016/j.gca.2018.09.010.

Usui A, Hino H, Suzushima D, Tomioka N, Suzuki Y, Sunamura M, Kato S, Kashiwabara T, Kikuchi S, Uramoto GI, Suzuki K, Yamaoka K. 2020. Modern precipitation of hydrogenetic ferromanganese minerals during on-site 15-year exposure tests. Sci Rep **10:**1–10. doi:10.1038/s41598-020-60200-5.

Van Dover CL. 1995. Ecology of Mid-Atlantic Ridge hydrothermal vents. Geol Soc Spec Publ **87:**257–294. doi: 10.1144/GSL.SP.1995.087.01.21.

Van Dover CL, Biscoito M, Gebruk AV, Hashimoto J, Tunnicliffe V, Tyler PA, Desbruyéres D. 2006. Milestones in the discovery of hydrothermal-vent faunas. Denisia **18:**13–25.

Varfolomeeva M, Artemieva A, Shunatova N, Yakovis E. 2008. Growth and survival of barnacles in presence of co-dominating solitary ascidians: growth ring analysis. J Exp Mar Bio Ecol **363:**42–47. doi:10.1016/j.jembe.2008.06.012.

Walker G, Yule AB, Nott JA. 1987. Structure and function in balanomorph larvae. *In*: Southward AJ (ed). Barnacle Biology. A.A. Balkema, Rotterdam, The Netherlands, pp. 307–328.

Watanabe H, Kado R, Kaida M, Tsuchida S, Kojima S. 2006. Dispersal of vent-barnacle (genus *Neoverruca*) in the Western Pacific. Cah Biol Mar **47:**353–357.

Watanabe H, Kado R, Tsuchida S, Miyake H, Kyo M, Kojima S. 2004. Larval development and intermoult period of the hydrothermal vent barnacle *Neoverruca* sp. J Mar Biol Assoc United Kingdom **84:**743–745. doi: 10.1017/S0025315404009841h.

Wheeler AJ, Murton B, Copley J, Lim A, Carlsson J, Collins P, Dorschel B, Green D, Judge M, Nye V, Benzie J, Antoniacomi A, Coughlan M, Morris K. 2013. Moytirra: Discovery of the first known deep-sea hydrothermal vent field on the slow-spreading Mid-Atlantic Ridge north of the Azores. Geochemistry, Geophys Geosystems **14:**4170–4184. doi:10.1002/ggge.20243.

Yamaguchi T, Newman WA. 1990. A New and Primitive Barnacle (Cirripedia: Balanomorpha) from the North Fiji Basin Abyssal Hydrothermal Field, and Its Evolutionary Implications. Pacific Sci **44:**135–155.

Yamaguchi T, Newman WA. 1997a. *Eochionelasmus paquensis*, New Species (Cirripedia: Balanomorpha), From 17°25'S, North of Easter Island: First Record of a Sessile Hydrothermal Barnacle From the East Pacific Rise. J Crustac Biol **17:**488–496. doi:10.2307/1549443.

Yamaguchi T, Newman WA. 1997b. The hydrothermal vent barnacle *Eochionelasmus* (Cirripedia, Balanomorpha) from the North Fiji, Lau and Manus Basins, South-West Pacific. Zoosystema **19:**623–649.

Yorisue T, Chan BKK, Kado R, Watanabe H, Inoue K, Kojima S, Høeg JT. 2016. On the morphology of antennular sensory and attachment organs in cypris larvae of the deep-sea vent/seep barnacles, *Ashinkailepas* and *Neoverruca*. J Morphol **277:**594–602. doi:10.1002/jmor.20522.

Yorisue T, Kado R, Watanabe H, Høeg JT, Inoue K, Kojima S, Chan BKK. 2013. Influence of water temperature on the larval development of *Neoverruca* sp. and *Ashinkailepas seepiophila* - Implications for larval dispersal and settlement in the vent and seep environments. Deep Res Part I Oceanogr Res Pap **71:**33–37. doi: 10.1016/j.dsr.2012.10.007.

Young P. 1998. Cirripedia (Crustacea) from the Campagne Biaçores in the Azores region, including a generic revision of Verrucidae. Zoosystema **20:**31–92.

Young P. 2001. Deep-sea Cirripedia Thoracica (Crustacea) from the northeastern Atlantic collected by French expeditions. Zoosystema **23:**705–756.

Zullo VA, Baum GR. 1979. Paleogene barnacles from the coastal plain of North Carolina (Cirripedia, Thoracica). Southeast Geol **20:**229–246.

Supplementary materials

Table S1. Morphometric measurements of carinal parietal plates from 69 specimens of *Bathylasma hirsutum*. (download)

Table S2. Applied Rpackages to plot the morphometric measurements. (download)

Table S3. Components of master mix cocktails used to perform PCR reactions. (download)

Table S4. Thermal cycling conditions of the polymerase chain reactions. Reaction steps are: 1 Initial denaturation, 2 Denaturation, 3 Annealing, 4 Elongation, 5 Final extension, 6 Cooling. Temperatures marked with an asterisk were used for the EF1 gene locus. (download)

Table S5. List of GenBank accession numbers for 146 novel *COI* and 141 novel EF1 1211 sequences of *Bathylasma hirsutum*. (download)